Radial Basis Functions Neural Networks for Nonlinear Time Series Analysis and Time-Varying Effects of Supply Shocks

Nobuyuki Kanazawa*

Department of Economics,
Soka University

March 17, 2020

Abstract

I propose a flexible Radial Basis Functions (RBFs) Artificial Neural Networks method for studying the time series properties of macroeconomic variables. To assess the validity of the RBF approach, I conduct a Monte Carlo experiment using the data generated from a nonlinear New Keynesian (NK) model. I find that the RBF estimator can uncover the structure of the NK model from the simulated data of 300 observations. Finally, I apply the RBF estimator to the quarterly US data and show that the positive supply shocks have significantly weaker expansionary effects during the periods of passive monetary policy regimes.

Keywords: Nonlinear Vector-Autoregression models; Radial Basis Functions; Zero Lower Bound; DSGE models; Supply Shocks.

JEL Classification: C45; E31.

*Email: nkanazawa@soka.ac.jp. Address: 1-236, Tangi-machi, Hachioji-shi, Tokyo, 192-8577, Japan. Phone: +81-42-691-9502. This paper was developed during my time at Cornell University as a PhD student and at the Hitotsubashi Institute for Advanced Study (HIAS) as a post-doc. I would especially like to thank Karel Mertens, Levon Barseghyan, and Christopher Huckfeldt for their great guidance and support. I would also like to thank Manabu Asai, Etsuro Shioji, Hiroshi Morita, the co-editor, an anonymous referee, seminar participants at the CFE conference (2017, London) and SNDE conference (2018, Tokyo) for very helpful comments and suggestions. All remaining errors are mine. I acknowledges the financial support from the Japan Ministry of Education, Culture, Sports, Science, and Technology, Japan Society for the Promotion of Science (JSPS KAKENHI Grant Number 20810914)

1 Introduction

In this paper, I use the Radial Basis Function (RBF), which is a class of Artificial Neural Network (ANN), as a nonlinear Vector Autoregression (VAR) estimator and examine its applicability to macroeconomic time series analysis. The RBF has been studied extensively in fields of computer science and neural networks, and it has been shown that the RBF can approximate any continuous functions on a compact domain (known as the universal approximation property).[1] The use of RBF in the macroeconomic time series analysis is motivated by its ability to flexibly estimate a nonlinear data-generating process without prior modeling of the type of nonlinearity. Despite its flexibility, however, the RBF can be efficiently estimated by following a simple two-step procedure commonly adopted in the neural network community that essentially breaks down a costly nonlinear estimation into a fast clustering method and a linear estimation.[2] The benefit of low computational costs allows researchers to estimate nonlinear VAR models having a typical amount of linear VAR dimensions. In this paper, I introduce the RBF application to macroeconometrics and show that the RBF time series model estimated via two-step estimation can be a valid alternative to other nonlinear estimators for macroeconomic time series analysis.

To validate the use of the RBF estimator for macroeconomic analysis, we must first test to see if the estimator can correctly capture the structure of the aggregate economy with a number of observations that is usually available to a macro-econometrician. This is because, even though the RBF estimator has the universal approximation property, its rate of convergence generally depends on the smoothness of the function to be approximated and the number of available observations. To this end, I conduct a Monte Carlo experiment using simulated time series data generated from a medium-scale nonlinear New Keynesian (NK) model, which economists and policy makers frequently view as a representation of the aggregate economy. Nonlinearity in this NK model comes from a kink in the central bank's monetary policy rule, wherein the interest rate is bounded from below at 0%. I then calculate the within-sample Mean-Squared-Errors (MSEs), which are defined by the distance between the true impulse responses from the NK model and the impulse responses estimated by the RBF estimator. For comparison, I also compute the MSEs using linear- and threshold-VAR (TAR) estimators. I find that the RBF estimator produces smaller MSEs than linear VARs and TARs, especially in middle and long horizons, even when the sample size is limited to

[1] See Hartman, Keeler, and Kowalski (1990) and Park and Sandberg (1991).

[2] This procedure is called 'unsupervised learning' in the neural nets field.

300 periods. The result suggests that the use of the RBF estimator for macroeconomic time series analysis may be appropriate.

I finally use the RBF estimator to understand the dynamic relationship between seven US macroeconomic variables from 1978 to 2016. Using the utilization-adjusted total factor productivity (TFP) of Fernald (2014) as a series of exogenous shocks, I estimate the impulse responses of output, consumption, investment, hours worked, expected inflation rate, and nominal interest rate. Through this exercise, I test the prediction of the textbook NK model, which states that the expansionary effects of a positive supply shock are weaker under passive monetary policy regimes, such as the zero-lower-bound (zlb) periods. Consistent with the NK model's prediction, I find that the effects of the positive TFP shock are considerably weaker during periods of zlb.

Furthermore, the output responses to the supply shocks are found to be similarly small between 2003 and 2004. During these periods, the federal funds rate was very low at around 1%. In fact, the estimated nominal interest rate response suggests that the Fed was not actively responding to supply shocks during these periods. Owning to the unresponsive nominal interest rate and the supply shocks' deflationary effects, I find that the real interest rate rises after the positive supply shocks during these periods, which discourages consumption, investment, and output. The finding highlights the critical role that the response of the real interest rate plays in shaping the responses of other macroeconomic variables. The study also suggests that the estimated responses of macroeconomic variables of 2003—2004 are remarkably similar to those during the zlb periods of 2008—2015.

My results contrast with those of Garín, Lester, and Sims (2019) and Wieland (2019), who found the strong expansionary effects of positive supply shocks during the periods of zlb. I briefly discuss potential explanations for the differences in the findings, and I show that these differences are a consequence of different data specifications rather than different methodologies. Specifically, I estimate the output response using the state-dependent local projection (LP) method and show that the effects of the supply shocks are considerably weaker during the zlb periods when the growth rate specifications are used and an outlier (2008Q4) is excluded. This exercise reiterates the point that macroeconomic dynamics during passive monetary policy regimes differ markedly from the macroeconomic dynamics typical of active monetary policy regimes, as prescribed by the basic NK model.

The rest of the paper is organized as follows: Section 2 reviews the literature on the RBF. Section 3 goes over the literature about time series analysis. Section 4 describes the Monte

Carlo simulation exercise. Section 5 illustrates an empirical application using the US data. Section 6 discusses the results, and Section 7 concludes.

2 Radial Basis Functions

In this paper, I focus on a particular class of ANN (i.e., the RBF). ANNs typically comprise several layers between input (independent) and output (dependent) variables. Each layer is made of multiple units, and a unit in one layer receives inputs from the previous layers, producing outputs for the succeeding layer. The RBF is characterized by having three layers with a single hidden layer in the middle and by having transformation functions in the hidden layer that form radial symmetry around the units.[3] Figure 1 shows a graphical description of the RBF. The three layers depicted in the figure are: (1) an input layer, where the independent variables enter the system; (2) a hidden layer, where the independent variables are transformed; and (3) a linear output layer, where the dependent variables are predicted. The RBF was first introduced as a solution technique for interpolation problems. During the late 1980s, the RBF formulation was extended to perform more general tasks of approximation.[4] Since then, a number of researchers, including Park and Sandberg (1991), Xu, Krzyżak, and Yuille (1994), and Girosi and Poggio (1990), have shown that any continuous function on a compact domain can be approximated arbitrarily well by the RBF.

2.1 RBF Formulation

Consider a univariate nonlinear autoregressive process, y_t, defined by $y_t = h(y_{t-1}) + \varepsilon_t$ $(t = 1, \ldots, N)$, where ε_t follows an independent and identical distribution (iid) with mean zero and constant variance. We assume that y_t is stationary and that $h(\cdot)$ is a nonlinear function. By definition, $h(y_{t-1})$ is the conditional expectation of y_t, given y_{t-1}. The RBF estimator for $h(y_{t-1})$ takes the following form:

$$\hat{h}(y_{t-1}) = \beta_0 + \sum_{j=1}^{M} D\left(\frac{||y_{t-1} - \xi_j||}{\lambda}\right)\beta_j, \tag{1}$$

[3] The word "hidden" is used to distinguish the layer in the middle from the input and output layers.
[4] See Broomhead and Lowe (1988), Moody and Darken (1989), and Poggio and Girosi (1990).

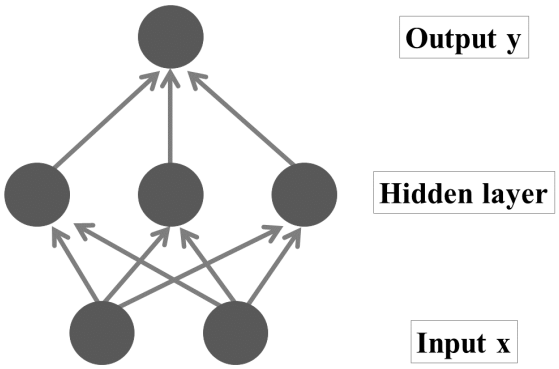

Figure 1: Graphical description of RBF

where ξ_j represents a unit (or a centroid) in the hidden layer for $j = \{1, \ldots, M\}$, M denotes the number of centroids, λ is a scale parameter, and β_0, β_1, ..., and β_M are scalar parameters. I choose the Gaussian density function for the kernel, $D(x) = \exp(-x/2)$, because it is a popular choice of base function for the RBF. Roughly speaking, when a new input enters the system, the RBF computes the Euclidean distance between the input and each of the centroids, ξ's. When, for instance, the distance between the input and j-th centroid, ξ_j, is smaller, the kernel (Gaussian density function) centering on that centroid assigns a larger weight, which activates β_j more strongly. The RBF computes the predicted value, $\hat{y}_t$, based on the weighted combinations of all the β's.

I now extend Equation 1 to a general case that permits multiple variables and lags. Let $\mathbf{y}_t$ be a $K \times 1$ vector of stationary nonlinear time series given by:

$$\mathbf{y}_t = H(\mathbf{x}_{t-1}) + \boldsymbol{\varepsilon}_t,$$

where $\mathbf{x}_{t-1} = (\mathbf{y}'_{t-1}, \ldots, \mathbf{y}'_{t-p})'$ is a $KP \times 1$ vector, and $\varepsilon_{\mathbf{t}}$ is an iid with mean $\mathbf{0}$ and finite covariance matrix. We may use an RBF estimator of order P (referred to as a RBF(P) model) defined by:

$$\hat{H}(\mathbf{x}_{t-1}) = \boldsymbol{\beta}_0 + \sum_{j=1}^{M} G(\mathbf{x}_{t-1}|\boldsymbol{\xi}_j, \boldsymbol{\lambda})\boldsymbol{\beta}_j, \tag{2}$$

where $\boldsymbol{\beta}_j$ and $\boldsymbol{\xi}_j$ $(j = 1, \ldots, M)$, $\boldsymbol{\beta}_0$, and $\boldsymbol{\lambda}$ are $K \times 1$ vectors. The kernel density function is given by:

$$G(\mathbf{x}_{t-1}|\boldsymbol{\xi}_j, \boldsymbol{\lambda}) = \exp\left\{-\frac{1}{2}\left(\mathbf{x}_{t-1} - (\mathbb{1}_{(P\times 1)} \otimes \boldsymbol{\xi}_j)\right)' (I_P \otimes \Lambda^{-1}) \left(\mathbf{x}_{t-1} - (\mathbb{1}_{(P\times 1)} \otimes \boldsymbol{\xi}_j)\right)\right\}, \quad (3)$$

with a diagonal matrix having $\Lambda = \text{diag}(\boldsymbol{\lambda})$. Here, $G(\mathbf{x}_{t-1}|\boldsymbol{\xi}_j, \boldsymbol{\lambda})$ measures the distances between each observation in $\mathbf{x}_{t-1}$ and the j-th centroid. Note that $\boldsymbol{\beta}_0$ represents a $K \times 1$ vector of constant coefficients and $\boldsymbol{\beta}_j$ denotes a $K \times 1$ vector of slope coefficients associated with the j-th centroid.

To estimate the three sets of parameters, $\boldsymbol{\xi}$'s, $\boldsymbol{\lambda}$, and $\boldsymbol{\beta}$'s, I must solve the following minimization problem:

$$\min_{\{\boldsymbol{\xi}_j, \boldsymbol{\beta}_j\}_{j=1}^{M}, \beta_0, \boldsymbol{\lambda}} \sum_{t=1}^{N} \left(\mathbf{y}_t - \hat{H}(\mathbf{x}_{t-1})\right)' \left(\mathbf{y}_t - \hat{H}(\mathbf{x}_{t-1})\right) \quad (4)$$

At first glance the problem appears complex and highly nonlinear. However, in Section 2.2, I show that this minimization problem can be solved quickly as if it were a linear optimization problem.

2.2 Parameter Estimation Methods and Renormalization

As specified in Section 2.1, there are three types of parameters that must be estimated: centroids $\boldsymbol{\xi}$'s, scale parameters $\boldsymbol{\lambda}$, and $\boldsymbol{\beta}$'s. The rate of convergence and the accuracy of the solution generally depend on the method of estimation. Because this paper does not aim to find the optimal method of estimation, I simply choose one of the popular estimation methods that break down the complex nonlinear minimization problem into two simple steps.[5]

In the two-step estimation, the parameters in the hidden layer ($\boldsymbol{\xi}$'s and $\boldsymbol{\lambda}$) and the $\boldsymbol{\beta}$'s are estimated separately. Note that, ideally, the global solution method[6] would be preferable. However, in reality, such methods exponentially increase the computational costs. Instead, I employ a two-step estimation that greatly reduces the computational costs and show that

[5]This method of training is also called "unsupervised training,"

[6]In the neural networks literature this method is called "supervised training," wherein the back-propagation is activated.

Figure 2: Illustration of K-means clustering

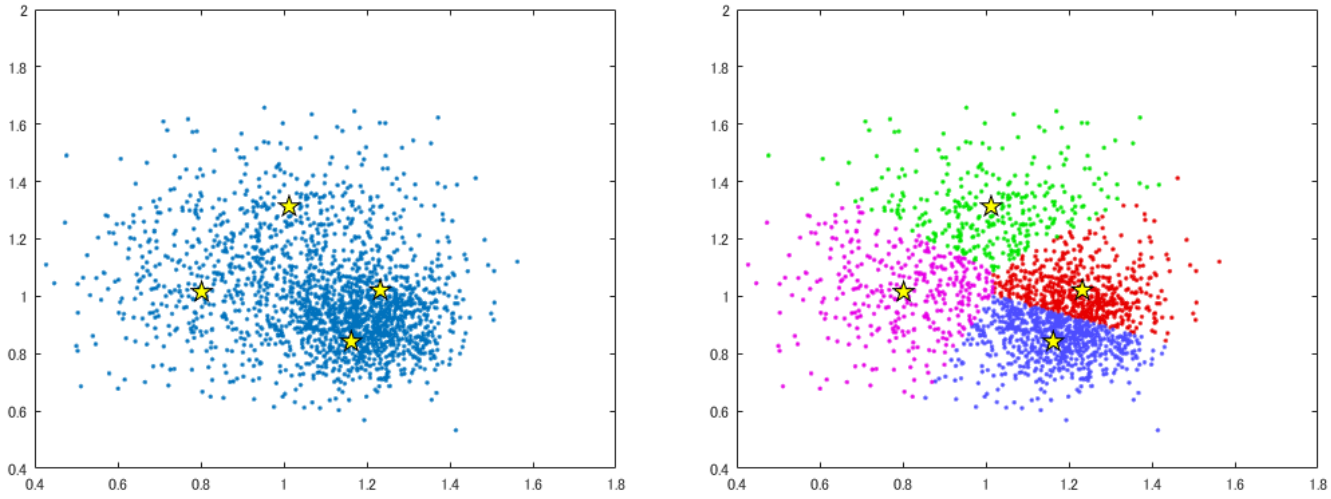

(a) Observations and "Means"

(b) Clusters

even with the simple two-step procedure, the RBF estimator performs competently compared to other traditional macroeconomic time series models. The two-step procedure is as follows. First, I employ a clustering method to fix the value of centroids, $\boldsymbol{\xi}_j$, and choose $\boldsymbol{\lambda}$. Second, I estimate $\boldsymbol{\beta}$'s in an ordinary least-square (OLS) manner.[7]

Regarding the first step, a common choice to fix centroids is employing the K-means clustering method. With this method, n observations are assigned into k clusters, with each observation belonging to the cluster that has the nearest mean. The mean of each cluster constitutes a prototype of that cluster, and for this reason, I use the means of the K-means clustering method as the centroids in the RBF estimation. Figure 2 illustrates the K-means clustering method. In this illustration, 1,000 observations are partitioned into four clusters with yellow stars representing the means of each cluster. Essentially, the RBF estimator constructs kernels (Gaussian density functions) around these centriods. The K-means clustering method offers a fast algorithm for picking centroids that are balanced representations of the entire sample.

Generally, centroids determined by K-means clustering are not unique, and the location of the centroids depends on the initial values. Therefore, I conduct a primitive, random search

[7]The drawback of these approaches is that the choice of location parameters do not reflect the conditional distribution, $Pr(\mathbf{Y}|\mathbf{X})$.

optimization by simply repeating the K-means clustering algorithm using 1,000 different initial values and by selecting a set of centroids that minimizes Equation 4. Other centroid-selection methods, including the orthogonal least square algorithm by Chen, Cowan, and Grant (1991) are considered. However, the crude optimization of the random search over different initial values repeatedly produce lower errors and is more stable.

In addition to the centroids, the scale parameters, $\boldsymbol{\lambda}$, must be estimated. I fix $\boldsymbol{\lambda}$ to be the variance of corresponding variable in $\mathbf{y}_t$ so that the kernel of the RBF in Equation 1 is akin to the standard normal density function. Fixing $\boldsymbol{\lambda}$ is convenient for computational efficiency. However, it has a side-effect of leaving hole-regions in the input space where no kernel has appreciable support. For example, the top panel of Figure 3 depicts the hole-regions and the support from the RBF kernels. Because $\boldsymbol{\lambda}$ is fixed, the kernel's width is also fixed, leaving a region where no kernel support can be reached. To avoid this problem, Friedman, Hastie, and Tibshirani (2008) suggested the use of the renormalized RBF, defined as:

$$\tilde{H}(\mathbf{x}_{t-1}) = \sum_{j=1}^{M} \tilde{G}_j \boldsymbol{\beta}_j^r \tag{5}$$

where[8]

$$\tilde{G}_j = G(\mathbf{x}_{t-1}|\boldsymbol{\xi}_j, \boldsymbol{\lambda}) \Big/ \sum_{m=1}^{M} G(\mathbf{x}_{t-1}|\boldsymbol{\xi}_m, \boldsymbol{\lambda}). \tag{6}$$

The bottom panel of Figure 3 illustrates the kernel support using the renormalized RBF, which is now extended to cover the entire region. I use the renormalized RBF for the remainder of the paper.

A convenient property of RBF implies that, after $\boldsymbol{\xi}$'s and $\boldsymbol{\lambda}$ are fixed, the function is linear in $\boldsymbol{\beta}^r$'s as shown in Equation 5. Thus, for the second step in the two-step estimation procedure, $\boldsymbol{\beta}^r$'s are estimated in the usual OLS manner.

Finally, following Blake and Kapetanios (2003), I use the Bayesian information criteria (BIC) to choose the number of centroids, M.[9]

[8]The renormalized RBF does not have an intercept for including it causes perfect collinearity.

[9]I also compute the Akaike information criteria, but BIC gives a clearer indication of the optimal number of centroids.

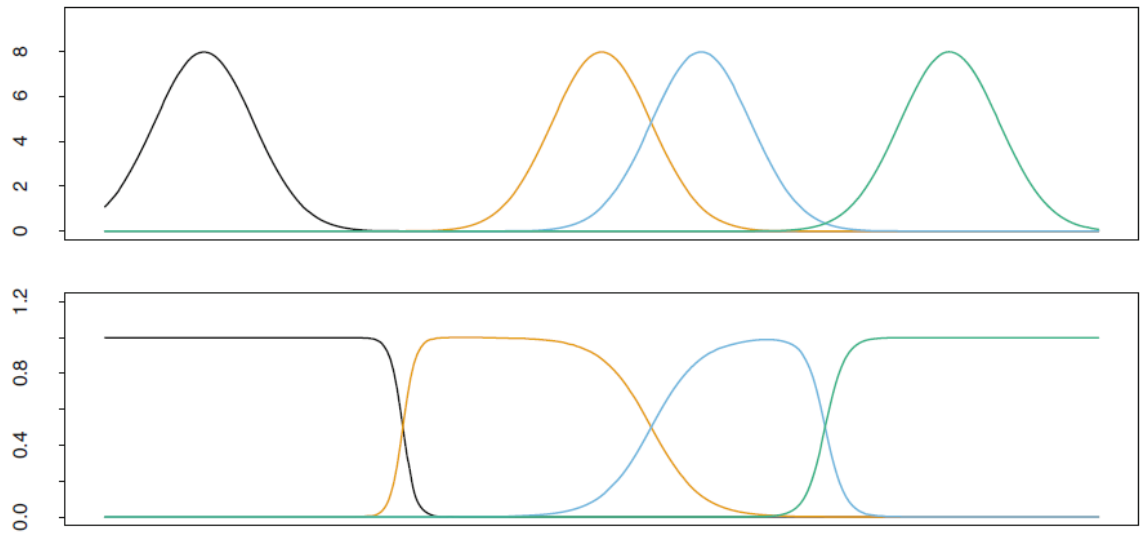

Figure 3: Top panel: RBF. Bottom panel: Nomalized RBF
(reprinted from Friedman, Hastie, and Tibshirani (2008)).

3 Literature Review

This paper is related to extensive literature on nonlinear time series models used for macroeconomic analysis. In this section, I highlight two principal approaches to parametric nonlinear estimation, review the literature on nonparametric estimation, discuss literature that directly estimates the impulse response functions, and list other papers that have applied ANN and machine learning techniques for economic analysis.

The first approach of capturing nonlinearities using parametric models relied on the use of regime-switching VAR models, including the TARs (e.g., Hubrich and Teräsvirta (2013), Balke and Fomby (1997), Teräsvirta, Tjøstheim, Granger, et al. (2010), Rothman, Van Dijk, and Hans (2001), Camacho (2004), and Galvao and Marcellino (2014)) and Markov-switching VARs (e.g., Krolzig (2013), Hamilton (1989), Sims, Waggoner, and Zha (2008), and Sims and Zha (2006)). These models are well-suited to describe correlated data that show clear dynamic patterns during different time periods characterized by different regimes. Additionally, recent approaches, such as the multiple change-point model of Koop and Potter (2007), have added more flexibility to these types of models by introducing an estimation method for regime-switching models where the number of regimes can be estimated.

The second and more related approach consists of the TVC-VAR models (Canova (1993),

Canova and Gambetti (2009), Cogley and Sargent (2001), Cogley and Sargent (2005), Primiceri (2005), Koop, Korobilis, et al. (2010), Koop, Leon-Gonzalez, and Strachan (2009)), which can capture general nonlinear dynamics by allowing for flexible variation in VAR coefficients. In a similar pursuit, this paper contributes to the literature by introducing the application of the RBF to the macroeconometrics that can handle the flexible estimation of nonlinear models.

Compared to the TVC-VAR literature, the RBF estimator has two limitations. First, the RBF estimator in this paper can only be applied to small- and moderate-dimensional models. The number of dimensions that can be handled using the RBF estimator is same as what is typically allowed for linear VARs estimation at this stage. This is in contrast to recent TVC-VAR literature (Koop and Korobilis (2013), Petrova (2019), and Chan, Eisenstat, and Strachan (2020)) that has introduced estimations and specifications that permit the use of large-dimensional TVC-VAR models (as large as 25 variables). Another limitation is that the RBF estimator does not admit the time-varying volatility at this stage, in contrast to the TVC-VARs introduced by Cogley and Sargent (2005) and Primiceri (2005) that permitted the time-varying volatility. This implies that, in case the assumption of constant volatility is violated, the RBF estimator is mis-specified. Despite these limitations, the current paper shows that the RBF estimator is promising in terms of macroeconomic time series analysis and serves as a starting point for incorporating the RBF techniques in macroeconometics.

The listed literature focused on parametric nonlinear estimation. However, there has also been extensive work on nonparametric estimation.[10] Local smoothing method was proposed by Robinson (1983), Härdle and Tsybakov (1997) and Härdle, Tsybakov, and Yang (1998). Additionally, an additive nonparametric VAR model was suggested by Jeliazkov (2013). The semi-nonparametric approach suggested by Gallant and Tauchen (1989) used Hermite expansions to approximate the one-step-ahead conditional density of time series data. A common challenge faced by those works is the curse of dimensionality, which limits their applicability. The RBF estimator can be useful in this context because of the low computation cost required for estimation when two-step estimation is used.

In addition to approaches that capture nonlinearity in time series data using the full-fledged VAR model mentioned above, there has been a growing interest in directly estimating the impulse response functions. This approach was pioneered by Jordà (2005), who proposed the LP method. This method can easily capture nonlinearities in the response functions,

[10] A comprehensive references can be found in Härdle, Lütkepohl, and Chen (1997)

but, as pointed out by Barnichon and Matthes (2018), the method posed serious difficulties of efficiency. Indeed, drawing inferences on a rich set of nonlinearities, including sign- and state-dependence, using the LP method is often difficult.

Recently, an improvement to this approach was suggested by Barnichon and Matthes (2018), who used few numbers of Gaussian functions to approximate the impulse functions. Like Jordà (2005), this approach was robust to a functional-form assumption error, but it had the advantage of reducing efficiency costs, because, rather than using the model-free estimation, they imposed a flexible parametric assumption based on a mixture of Gaussian base functions. Like Barnichon and Matthes (2018), this paper utilizes the Gaussian functions to approximate macroeconomic dynamics. However, the current paper differs from Barnichon and Matthes (2018) in two respects. First, this paper uses a mixture of Gaussian base functions to capture nonlinear time series as a full-fledged VAR model. Their approach directly estimated the impulse response functions. Second, this paper employs a neural network structure, making use of the hidden layer. The multiple-layer structure of the RBF provides extra flexibility, making it possible for its estimator to generically work in many different applications without prior modeling of nonlinearity types or without specifying how states switch.

In addition to the nonlinear time series literature listed above, the current paper is obviously related to the literature that employed ANN for economic and financial time series analysis. Most the research that applied ANNs to economics focused on forecasting financial variables. In these studies, the ANN models were often found to outperform traditional time series models.[11] Fewer studies have tested ANN's ability to forecast macroeconomic variables. Swanson and White (1997) applied ANN models to forecast nine US macroeconomic series and concluded that although their results were mixed, the ANN models were promising even when no explicit nonlinearity was found in the macroeconomic dynamics. Moshiri and Cameron (1999) investigated whether an ANN could correctly forecast inflation, and Tkacz (2001) used it to forecast the Canadian GDP. An extensive review of the use of ANN in the context of economic analysis was presented by Kuan and White (1994). Recent applications of machine learning in economic forecasting were described by Guerrón-Quintana and Zhong (2017). Fernández-Villaverde, Hurtado, and Nuno (2018) used the machine learning technique to solve a nonlinear dynamic macroeconomic model. Blake and Kapetanios (2000), Blake and Kapetanios (2003), Blake and Kapetanios (2007a), and Blake and Kapetanios

[11] See Hutchinson, Lo, and Poggio (1994), Lachtermacher and Fuller (1995), Zhang and Wan (2007), Zhang and Hu (1998), and Guresen, Kayakutlu, and Daim (2011).

(2007b) used the RBF for a variety of specification testing problems. In contrast to these papers, the current paper uses the ANN technique to model macroeconomic time series data as a full-fledged VAR model and investigates the dynamic relationships between macroeconomic variables using impulse response functions.

4 Monte Carlo Simulation

To study the validity of the RBF estimator for macroeconomic time series analysis, I report on a Monte Carlo simulation in this section. I ask, "If the true data-generating process of an economy is a medium-sized nonlinear NK model, can RBF networks uncover its structure from a simulated dataset?" To answer this question, I must first solve a nonlinear NK model globally, and I then simulate data using this NK model. The nonlinearity of this NK model stems from the kink in the central bank's Taylor rule, in which the bank cannot lower the interest rate below zero. In Appendix 8.1, I describe in detail the NK model that is used for simulation. After I solve the model, I simulate the time series data for 1 million periods. The nominal interest rate hits zero for about 1.85% of the simulated periods.

Using the time series data generated by the NK model, I calculate the within-sample MSEs of the impulse responses estimated by the RBF estimator, the linear VARs, and the two-regime TARs. Then, I compare the performance of the RBF estimator against the other two estimators. The MSEs are measured using the deviation of the estimated impulse responses from the true impulse responses produced by the NK model. I present the MSEs under two different scenarios. In the first scenario, the economy is in a normal state, in which the nominal interest rates are strictly positive. To confirm that the economy is far from the zlb state, I ensure that the nominal interest rate is greater than 1% during at least five consecutive periods before and after the shock hits the economy. The second scenario considers the economy under the zlb state, in which the nominal interest rate is bound at zero when the shock hits the economy.

The exogenous state variable for the NK economy is the productivity shock, a_t, and the endogenous state variables are price dispersion, consumption, and interest rate. Because econometricians typically do not have a good measure of price dispersion, I assume that I observe the inflation rate rather than the price dispersion. Because a_t is orthogonal to the other variables, I impose the assumption that the productivity shock can affect the other variables contemporaneously but not vice versa. Next, I describe the three estimators used

for the MSE comparison.

4.1 Model Description

4.1.1 RBF estimator

Let π_{t+1} be inflation, C_t be consumption, R_t be interest rates, and $\mathbf{X}_t = [\pi_{t+1},\ C_t,\ R_t]$. Our RBF estimator can be written as follows:

$$\mathbf{X}_t = \tilde{H}\left(a_t, \{a_{t-p}, \mathbf{X}_{t-p}\}_{p=1}^{P}\right) + \Omega_R^{1/2} e_t^{\mathbf{X}} \tag{7}$$

where $e_t^{\mathbf{X}}$ denotes the structural shocks to $\mathbf{X}_t$.

4.1.2 Linear VAR

Let $\mathbf{Y}_t = [a_t,\ \pi_{t+1},\ C_t,\ R_t]$. I impose the same assumption as the one made for RBF estimator above in which the productivity shock is exogenous and affects other variables contemporaneously but not vice versa by ordering a_t at the very first. The linear VAR is as follows:

$$\mathbf{Y}_t = A_0 + \sum_{p=1}^{P} A_p \mathbf{Y}_{t-p} + \Omega_V^{1/2} e_t^{\mathbf{Y}} \tag{8}$$

with A_0 and A_p for $p = \{1, \ldots, P\}$ representing matrices of VAR coefficients and $e_t^{\mathbf{Y}}$ denoting the structural shocks to $\mathbf{Y}_t$.

4.1.3 TAR

Lastly, I estimate the two-regime TAR model defined as

$$\mathbf{Y}_t = \left[c_1 + \sum_{p=1}^{P} \Gamma_{1,p} \mathbf{Y}_{t-p} + \Omega_1^{1/2} e_t^{\mathbf{Y}}\right] S_t + \left[c_0 + \sum_{p=1}^{P} \Gamma_{0,p} \mathbf{Y}_{t-p} + \Omega_0^{1/2} e_t^{\mathbf{Y}}\right] (1 - S_t) \tag{9}$$

where

$$S_t = \{0, 1\} \text{ and } S_t = 1 \text{ if } R_{t-d} > R* \tag{10}$$

The TAR model considers the possibility of two regimes, in which a regime switches when the d-th lag of the interest rate, R_{t-d}, exceeds a threshold value, $R*$. I assume that both

d and $R*$ are unknown parameters that need to be estimated. The model is designed to capture the structure of the NK economy in the normal state ($S = 1$) and in the zlb state ($S = 0$). Note that $c_1, c_0, \Gamma_{1,p}$, and $\Gamma_{0,p}$ are the matrices of coefficients for each state. I follow Alessandri and Mumtaz (2017) for the estimation of Equation 9 and 10. The procedure is described in Appendix 8.6.

4.2 Generalized Impulse Response

One complication arises when I estimate nonlinear impulse response functions, which generally depend on future shocks, the current state of the economy (history), and the sign and magnitude of the current shock. To accommodate the impulse responses to various future shocks, I use the generalized impulse response functions in the spirit of Koop, Pesaran, and Potter (1996).[12] Let GI denote a generalized impulse response function. Then the impulse response of a variable, $\mathbf{Y}_{t+h}$, during h-period ahead is:

$$GI(h, v_t, \omega_{t-1}) = E[\mathbf{Y}_{t+h}|v_t, \omega_{t-1}] - E[\mathbf{Y}_{t+h}|\omega_{t-1}] \quad \text{for } h = 0, 1, \ldots \tag{11}$$

where v_t is the structural shock to a_t, and ω_{t-1} is the history ($\omega_{t-1} = \{a_{t-p}, \mathbf{X}_{t-p}\}_{p=1}^{P}$ for the RBF, and $\omega_{t-1} = \{\mathbf{Y}_{t-p}\}_{p=1}^{P}$ for the other two estimators). The examples of the generalized impulse responses using the RBF estimator, with the confidence bands computed by residual-based block bootstrap method, are illustrated in Appendix 8.7.

4.3 Results: MSE Comparison

To assess the overall performance and accuracy of the RBF estimator, I present below the within-sample MSEs. For comparison, I also present the MSEs produced by the linear VAR with four lags (VAR(4)) and the TAR with two lags (TAR(2)). I employ one lag for the RBF estimator (RBF(1)). The MSEs are computed on the basis of 1,000 Monte Carlo simulations. In each simulation, I carry out the following procedures: randomly pick a new sample of 300 observations, estimate the RBF, linear VAR, and TAR models, select a history within that

[12] Earlier work includes Beaudry and Koop (1993), Potter (1995), Pesaran and Shin (1996), and Potter (2000). In the generalized impulse response framework, the problem of future shock-dependence is handled by averaging out the impulse responses with many different future shocks. I use the Monte Carlo integration to compute the conditional expectation, and I calculate the expectation by averaging out 1,000 different paths of simulated future shocks. See Koop, Pesaran, and Potter (1996) for more details.

sample, give a shock, estimate generalized impulse response functions, and compute the MSEs. In Table 1, I present the h-period ahead MSEs of inflation rate, consumption, and interest rates for the normal state.

Table 1: MSE Performance in normal state (estimation periods = 300)

	Inflation			Consumption			Interest rates		
	VAR(4)	TAR(2)	RBF(1)	VAR(4)	TAR(2)	RBF(1)	VAR(4)	TAR(2)	RBF(1)
$h = 1$	0.0394	0.1957	0.1750	0.0191	0.0699	0.1421	0.0206	0.0983	0.0425
$h = 3$	0.0411	0.1590	0.0593	0.0851	0.4366	0.1240	0.0256	0.0943	0.0256
$h = 5$	0.0407	0.0845	0.0271	0.1127	0.6251	0.1185	0.0256	0.0854	0.0205
$h = 10$	0.0214	0.0286	0.0059	0.1353	0.3055	0.0872	0.0260	0.0302	0.0159
$h = 15$	0.0094	0.0095	0.0018	0.1208	0.1138	0.0492	0.0214	0.0190	0.0086
$h = 20$	0.0039	0.0082	0.0006	0.0738	0.0494	0.0249	0.0118	0.0149	0.0043
$h = 30$	0.0015	0.0036	0.0001	0.0242	0.0136	0.0058	0.0041	0.0090	0.0010

Notes: Summary statistics over 1,000 Monte Carlo replications. MSE is the mean-squared error of the estimated impulse response function. A smaller MSE means that an estimator-produced impulse response is closer to the true structural impulse response. VAR(4), TAR(2), and RBF(1) indicate that the estimators used to produce the MSEs shown in corresponding columns are VARs with four lags, TARs with two lags, and RBF estimators with one lag.

As Table 1 show, the performance of the RBF estimator compared to the VAR and TAR are mixed. In the short horizon (1- and 3-period ahead MSEs), the RBF estimator produces larger errors compared with the linear VAR. However, in the middle-to-longer horizons (5-period ahead and longer), the RBF estimator produces the smallest MSEs compared to the other estimators. The result that the RBF estimator outperforms the linear VAR in the middle and longer horizons is striking given that the NK model can be well-approximated by linear functions in the normal state.

Table 2 shows the MSEs of inflation, consumption, and interest rates under the zlb state. For the zlb case, the errors from the RBF estimator when it predicts inflation and interest rates are lowest compared with the other estimators for all horizons. The RBF estimator for the 1-period ahead prediction of consumption produces larger errors compared to the linear VAR model. However, from the third period on, the errors from the RBF estimator is consistently lower than the other two estimators even for the consumption. The fact that the RBF estimator clearly outperforms the VAR and TAR models in the case of zlb suggests that the RBF estimator is useful for capturing nonlinear- and history-dependent dynamic responses of the macroeconomic variables that might not be captured in the VAR and TAR

Table 2: MSE Performance in zlb state (estimation periods = 300)

	Inflation			Consumption			Interest rates		
	VAR(4)	TAR(2)	RBF(1)	VAR(4)	TAR(2)	RBF(1)	VAR(4)	TAR(2)	RBF(1)
$h = 1$	0.4453	0.2894	0.2534	0.1272	0.1224	0.2679	0.1975	0.1202	0.1143
$h = 3$	0.1130	0.1502	0.0654	0.2294	0.3784	0.2008	0.0911	0.0827	0.0436
$h = 5$	0.0611	0.0837	0.0343	0.1466	0.5764	0.1299	0.0314	0.0768	0.0178
$h = 10$	0.0215	0.0261	0.0068	0.1352	0.3008	0.0813	0.0260	0.0286	0.0143
$h = 15$	0.0094	0.0088	0.0019	0.1209	0.1106	0.0483	0.0214	0.0164	0.0083
$h = 20$	0.0039	0.0074	0.0006	0.0738	0.0467	0.0247	0.0118	0.0128	0.0042
$h = 30$	0.0015	0.0032	0.0001	0.0242	0.0123	0.0058	0.0041	0.0078	0.0010

Notes: Summary statistics over 1,000 Monte Carlo replications. MSE is the mean-squared error of the estimated impulse response function. A smaller MSE means that an estimator-produced impulse response is closer to the true structural impulse response.

models.

Overall, the result in this section indicates that the RBF estimator can uncover the structure of the nonlinear NK model even from a small sample of simulated data and that the RBF estimator can be a useful alternative to the linear VAR and TAR models. The result also suggests that the use of the RBF estimator for macroeconomic time series analysis may be appropriate.

5 Application to the US Data

Finally, I apply the RBF estimator to the quarterly US data. Following Wieland (2019) and Garín, Lester, and Sims (2019), I ask if a positive supply shock is less expansionary when the nominal interest rate is at the zlb. The question is motivated by the textbook NK model, which predicts the possibility of a contractionary supply shock at the zlb. The mechanism that underlies this prediction is described below.

I assume that a positive supply shock is an increase in neutral productivity. First, an increase in productivity decreases the inflation rate and the equilibrium real interest rate. When such a shock hits the economy, the central bank reacts by lowering nominal interest rates following the Taylor rule in the normal state. However, if the economy is at the zlb, the central bank is unable to push down the nominal interest rate further. Consequently, the real interest rate will rise, and the demand will suffer. In the extreme case where the zlb

is expected to last for a long period, the increase in the real interest rate can potentially be so large that the negative demand response dominates the positive effect of the productivity shock. When that happens, the GDP decreases.

To test the predictions of the NK model, Wieland (2019) examined the experiences of the Great East Japan Earthquake and the oil-supply shocks and found that the effects of a supply shock remained the same at the zlb, in contrast to the NK model's prediction.[13] Garín, Lester, and Sims (2019), using the utilization-adjusted TFP shock estimated by Fernald (2014), found that a positive supply shock was even more expansionary at the zlb. Because their findings potentially cast doubt on the assumptions that underlie the NK models, I also employ the RBF estimator with the utilization-adjusted TFP shock estimated by Fernald (2014) to investigate this important question. Unlike previous studies, I find some evidence of weaker expansionary effects during passive monetary policy regimes.

5.1 Data

The dataset includes the following six variables: the log difference of real GDP, $\Delta \ln Y_t$; personal consumption, $\Delta \ln C_t$; private investment, $\Delta \ln I_t$; the log of hours worked, $\ln N_t$; the expected inflation rate from the University of Michigan's Survey of Consumers, π_t^e; and the effective federal funds rate, r_t.[14] In addition to these variables, I use the utilization-adjusted TFP process estimated by Fernald (2014).

Garín, Lester, and Sims (2019) illustrated that the utilization-adjusted TFP series proposed by Fernald (2014) could be considered an exogenous shock process. Garín, Lester, and Sims (2019) used four popular measures of exogenous macroeconomic shocks[15] and showed that these measures did not Granger cause the utilization-adjusted TFP shock. They concluded, therefore, that the utilization-adjusted TFP process could be treated as an exogenous shock process. Based on their evidence, I, too, treat the utilization-adjusted TFP process as an exogenous shock process.

[13] Wieland (2019) also suggested that the expansionary effects of a supply shock may be even larger at the zlb.

[14] Real GDP (GDPC09), personal consumption (PCEC), and private investment (FPI) are from the NIPA table. Hours are obtained by multiplying civilian employment (CE16OV) and average weekly hours duration (PRS85006023). The GDP, consuption, investment, and hours are expressed as per capita by dividing the variables by the civilian noninstitutional population (CNP16OV).

[15] The four measures are Romer and Romer (2004)'s monetary policy shocks, Romer and Romer (2010)'s tax shocks, Ramey (2011)'s defense news shock, and Kilian (2008)'s exogenous oil price shock.

The dataset begins in 1978Q1, when the quarterly data of inflation expectation became available, and it ends in 2016Q4. The US economy was in the zlb state from the last quarter of 2008 to the last quarter of 2015.

5.2 Generalized Impulse Responses

I next estimate the generalized impulse responses to a positive TFP shock. The estimated model is:

$$\mathbf{X}_t = \tilde{H}\left(\Delta \ln A_t, \{\Delta \ln A_{t-p}, \mathbf{X}_{t-p}\}_{p=1}^{P}\right) + u_t \tag{12}$$

with $\mathbf{X}_t = [\Delta \ln Y_t, \Delta \ln C_t, \Delta \ln I_t, \ln N_t, \pi_t^e, r_t]$ and u_t representing a white-noise reduced form error. I assume that the utilization-adjusted TFP shock can affect the other variables within the same period, but not vice versa. I set the lags to four.

As in Section 4.1, I define the generalized impulse response of a variable, $\mathbf{X}_{t+h}$, during the h-period ahead to be

$$GI(h, v_t, \omega_{t-1}) = E[\mathbf{X}_{t+h}|v_t, \omega_{t-1}] - E[\mathbf{X}_{t+h}|\omega_{t-1}] \text{ for } h = 0, 1, \ldots \tag{13}$$

with v_t denoting the structural shock to $\Delta \ln A_t$, $\omega_{t-1} = \{\Delta \ln A_{t-p}, \mathbf{X}_{t-p}\}_{p=1}^{P}$ representing the history, and t spanning from 1978Q1 to 2016Q4. I set the size of the shock, v_t, to one standard deviation of $\Delta \ln A_t$. Because $\Delta \ln A_t$ exhibits a strong fluctuation and because the estimated impulse responses depend on the current and past values of $\Delta \ln A_t$, the resulting impulse responses also exhibit significant fluctuations. To avoid this issue, the impulse responses shown below are averaged out over $[t-2, \ldots, t+2]$ for all t whenever possible. To estimate the impulse response functions, I impose the assumption that the shock to $\Delta \ln A_t$ affects the other variables contemporaneously but not vice versa.

Figure 5: Responses at different horizons

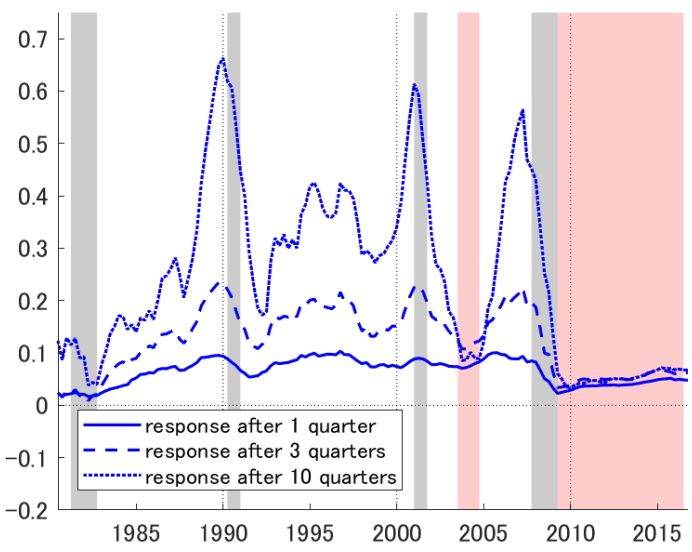

(a) cumulative GDP

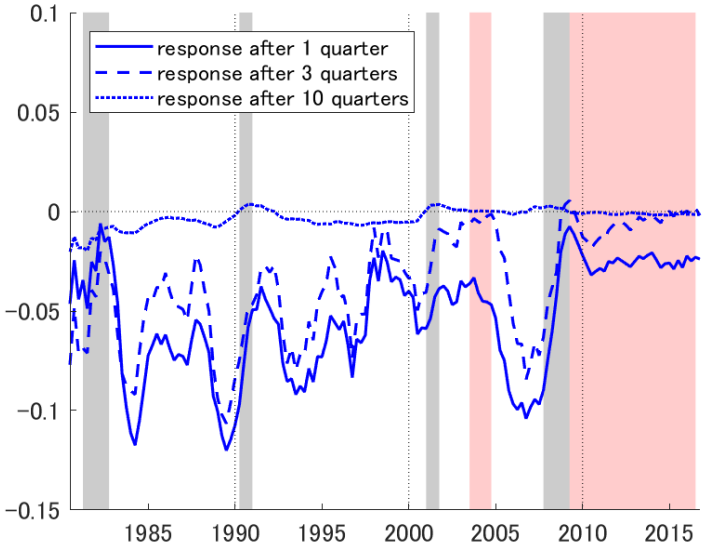

(b) Expected Inflation

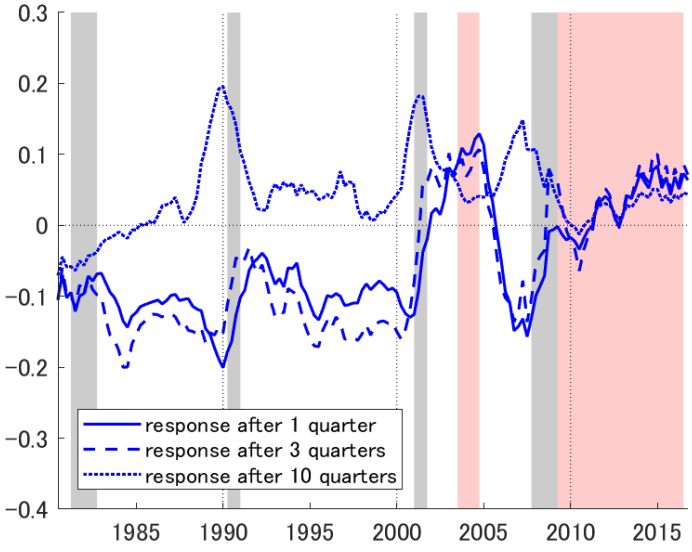

(c) Fed funds rate

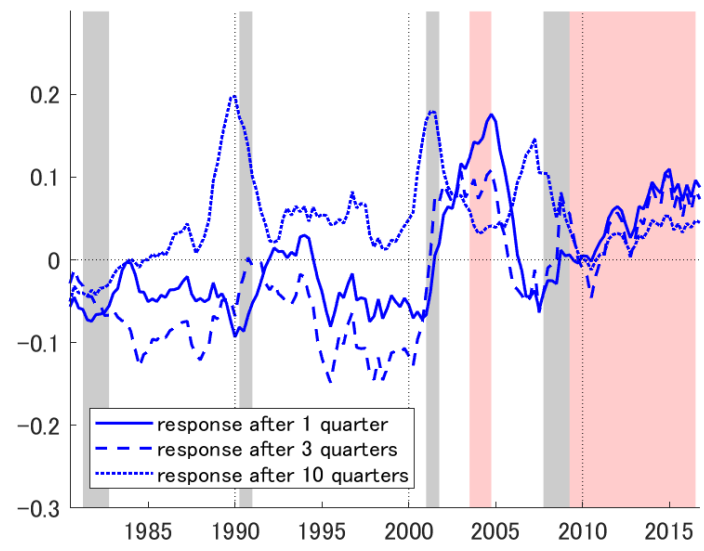

(d) real interest rate

Notes: Impulse response functions (in percent) to a one standard-deviation positive TFP shock after 1st, 3rd, and 10th quarters. Black shaded areas corresponds to NBER-recession dates. Red shaded areas represent the periods of weak output responses outside the recession dates.

Figure 6: Responses at different horizons

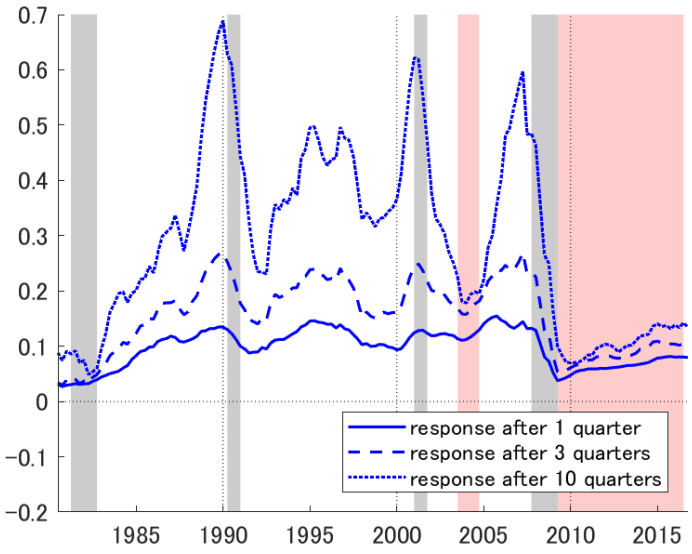

(e) cumulative Consumption

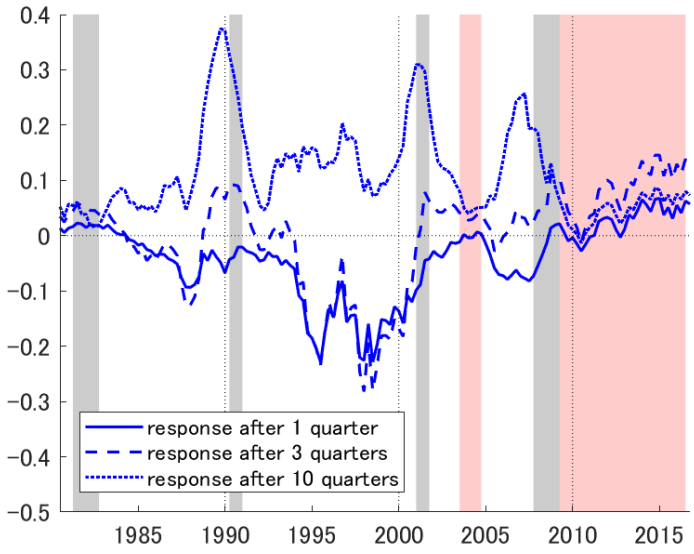

(f) Hours worked

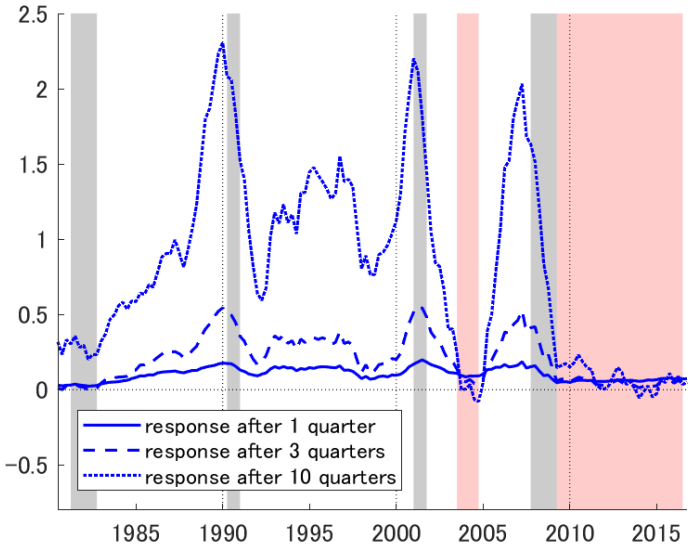

(g) cumulative Investment

Notes: Impulse response functions (in percent) to a one standard-deviation positive TFP shock after 1st, 3rd, and 10th quarters. Black shaded areas corresponds to NBER-recession dates. Red shaded areas represent the periods of weak output responses outside the recession dates.

5.3 Results

Figures 5-6 plot the point estimates of the responses after 1 quarter, 3 quarters, and 10 quarters between 1980 and 2016. In Figures 12-18 in Appendix 8.8, the impulse responses are shown with confidence bands for the horizons of the (1) 1st quarter, (2) 2nd quarter, (3) 5th quarter, and (4) 9th quarter.[16] In these figures, the point estimates are drawn in blue solid lines and the 68 percent confidence bands are expressed as red dotted lines

Generally, the impulse responses from the RBF estimator look reasonably sensible. The positive supply shocks have positive and persistent effects on output, consumption, and investment. Expected inflation declines immediately after the shock, but the effect is short lived. The Fed funds rate also decreases after the shock in most periods, which is consistent with the Taylor rule. Hours worked goes down during the first few quarters during most periods, but it rises over the longer horizon. Overall, these responses are consistent with previous studies that investigated the effects of supply shocks on macroeconomic variables. Nonetheless, the figures illustrate that there are substantial time variations in the responses of the macroeconomic variables.

Figure 5(a) shows the response of the cumulative GDP.[17] As summarized above, the TFP shock is expansionary during all periods but exhibits a substantial time-variation in terms of the magnitude of its effects. The supply shock's post-10-quarters effects vary from approximately 0 to 0.7%, depending on the timing of the shock. The figure also suggests that the effect of the productivity shock is procyclical. The 2008 financial crisis had a particularly powerful impact: it weakened the effects of the productivity shock, reducing its after-10-quarters effects from 0.57% in 2007Q2 to 0.05% in 2009Q4.

Surprisingly, the expansionary effects of the productivity shocks were considerably weaker during the zlb periods even after the recession that followed the 2008 financial crisis ended. These weak expansionary effects are characterized by the weak on-impact effects and the lack of persistence. Interestingly, similarly weak output responses are observed between 2003 and 2004, when the persistence of the effects was also absent. The decline of the output responses probably cannot be attributed to the procyclical effects of the supply shocks because these periods do not correspond to the recessionary periods. Rather, they correspond to the recovery phase from the 2001 recession, when the fed funds rate was kept very low at around

[16] The confidence bands are computed using the block bootstrap method.

[17] The result shown here is not the GDP difference. It is the cumulative sum of the estimated impulse responses.

1%, and to the periods right before the rate started to rise successively in 2005 and 2006.[18]

Figure 5(c) plots the estimated response of the fed funds rate. Although the interest rate is estimated to go down in most periods (consistent with the Taylor rule), it was estimated to either go up or stay the same between 2003 and 2004 and after the 2008 financial crisis.[19] Furthermore, Figure 5(d), which shows the response of the real interest rate calculated from the simple Fisher equation[20], indicates that the real interest rate would have been higher in response to the supply shock around 2003—2004 and after 2008. The results suggest that the response of the real interest rate plays a crucial role in the formation of the output responses. The fact that the supply shocks are found to have weaker expansionary effects not only during the zlb periods but also between 2003 and 2004 makes the prediction of the NK model, in which the monetary policy impotency reduces the effects of supply shocks, more convincing.

Figure 5(e) shows the response of cumulative consumption. Like output response, consumption tends to increase throughout the sample in response to the positive productivity shock. However, the response is particularly weak during 2003-2004 periods and after the 2008 financial crisis. Moreover, the cumulative investment response shown in Figure 5(g) exhibits particularly weak responses during the 2003—2004 period and after 2008. To reiterate, these findings are in accordance with the textbook NK model and the findings from the output and interest rates responses noted above. The decline of in inflation expectation with the unresponsive monetary policy raises the real interest rate and discourages consumption and investment.

Finally, Figure 5(f) plots the response of hours worked. Previous literature found that the hours worked decreased in the short run in response to a positive productivity shock, which is often referred to as evidence for price-stickiness in the macro models. My finding is consistent with the existing literature: the hours worked decrease in the short-run but rise over the longer horizon. This pattern is stable for most of the sample periods, with the exception of the recessionary periods during the early 1980s, the 2001—2005 periods, and after 2008. These periods correspond to the periods of a large slack in the labor market and to the periods of relatively small or positive real interest rate responses. Peculiarly, after

[18] see Figure 11.

[19] The responses during these periods are not statistically different from zero.

[20] The real interest rate = nominal interest rate - expected inflation. The negative real interest rate response means that the fed funds rate decreased for more than one-for-one in response to the decline in the expected inflation.

2008, the positive productivity shocks are estimated to increase the hours worked over both short and long horizons.

In summary, the estimated impulse responses from the RBF estimator suggest that the response of macroeconomic variables to a positive supply shock is substantially time variant. The responses also hint that the effects of the productivity shocks might have been quantitatively and qualitatively different after the recent financial crisis and the 2003—2004 periods, when the monetary policy was perhaps less sensitive to the deflationary pressure caused by the supply shocks. In particular, the effects of the supply shocks during the periods of monetary policy inaction are found to be considerably less expansionary, which is consistent with the textbook NK model but is inconsistent with what Wieland (2019) and Garín, Lester, and Sims (2019) reported. The findings indicate that the economic responses to the supply shocks around 2003-2004 were markedly similar to the responses during the zlb periods. Moreover, the findings highlight the critical role that the response of the real interest rate plays in determining the responses of other macroeconomic variables. Importantly, all of the findings described above are based on the RBF estimator, which was estimated without imposing a priori functional form assumption.

6 Discussion

Why do the estimates in Section 5 differ starkly from those found in the existing literature, which concludes that the supply shocks are even more expansionary under the zlb? Is the difference an artifact of the nontraditional methodology employed in this paper? To answer these questions, I briefly investigate the relationship between the TFP shocks and the output using the state-dependent LP method of Jordà (2005).

Using the same data that I used in Section 5, I estimated the following regression:

$$\begin{aligned}\sum_{j=0}^{h} \Delta \ln(\mathbf{Y}_{t+j}) =& (1 - Z_t)\left(\alpha_h^n + \beta_h^n \Delta \ln A_t + \phi_h^n(L)\mathbf{x}_{t-1}\right) \\ &+ Z_t\left(\alpha_h^z + \beta_h^z \Delta \ln A_t + \phi_h^z(L)\mathbf{x}_{t-1}\right) + u_{t+h}\end{aligned} \tag{14}$$

where Z_t is the indicator variable for the zlb periods, and $\mathbf{x}_t$ is the control variables. Following Garín, Lester, and Sims (2019), I define the zlb as the periods between 2008Q4 and 2015Q4.

The control variables are lagged $\Delta \ln \mathbf{Y}_t$ and $\Delta \ln A_t$. I set the number of lags to four. Because I do not need to use the expected inflation, I now extend the dataset to periods between 1948Q1 and 2016Q4. Additionally, I exclud the 2008Q4 because it nontrivially affects the estimated on-impact response of output during the zlb periods. The latter probably is caused by the large impact of the Lehman failure output, which is not driven by movement in the TFP.

Figure 7: Response of GDP using LP method

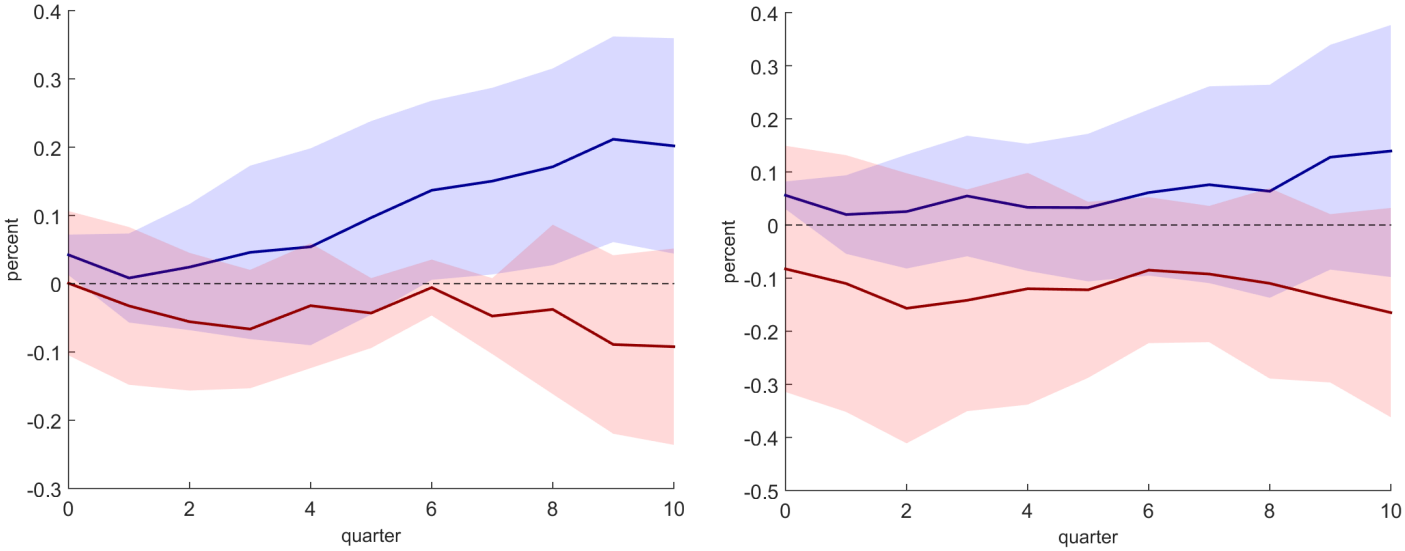

(a) Dependent variable: $\sum_{j=0}^{h} \Delta \ln \mathbf{Y}_{t+j}$

(b) Dependent variable: $\ln \mathbf{Y}_{t+h} - \ln \mathbf{Y}_{t-1}$

Notes: Estimated impulse response of output to a one unit TFP shock at various horizons. The solid blue line shows the response under the normal periods (i.e. when Zt = 0). The solid red line is the response when the ZLB binds (Zt = 1). The shaded bands represent the 90 percent confidence interval.

The left panel of Figure 7 shows the estimated cumulative output responses during the normal periods in the blue line and during the zlb periods in the red line. The shaded bands represent the 90 percent confidence interval. The output response during the normal periods is initially small, but it grows larger over time, culminating at around 0.2% in the 10th quarter. In contrast, the estimated response is weaker during the zlb periods and is not statistically different from zero for all horizons. The result is consistent with my finding in Section 5 that the weaker output response occurs when the monetary policy does not react actively to the shocks. As a robustness check, I also regress Equation 14 with the dependent variable specified as $(\ln \mathbf{Y}_{t+h} - \ln \mathbf{Y}_{t-1})$. The results shown in the right panel of Figure 7

indicate that the main conclusion stays the same.

In contrast to previous literature, which concluded that the expansionary effects of the supply shocks were even larger at the zlb, I find that the supply shocks become less expansionary during those periods. The difference is likely to be a product of different data specifications rather than of different methodologies. In particular, Garín, Lester, and Sims (2019) used aggregate GDP and the log-level specification, whereas I use the GDP per capita and the growth rate specification. Additionally, I also exclude the outlier (2008Q4). Once I treat the data as described, the supply shocks are found to have weaker expansionary effects during the passive monetary regimes even when I use the state-dependent LP method.

7 Conclusion

In this paper, I investigated the applicability of RBF to macroeconomic time series analysis. The RBF estimator is a useful alternative to traditional estimators because of its low computational costs, which allow researchers to estimate nonlinear VAR models with a dimensional size of what is typically allowed in linear VARs.

Based on a medium-scale nonlinear NK model, I performed a series of Monte Carlo experiments to study the small sample properties of the proposed RBF estimator. I found that the RBF estimator produced smaller MSEs than the linear VAR and TAR models, especially in terms of the middle- and long-period horizon. The generalized impulse responses from the RBF estimator suggested that the estimator can learn the structure of the nonlinear NK model from the sample of simulated data, whose lengths were as small as 300 periods.

Finally, by applying the RBF estimator to quarterly US data, I found that the responses of macroeconomic variables to a positive supply shock exhibited substantial time variations. The result suggested that the expansionary effects of a supply shock became significantly weaker during periods of monetary policy inaction, which is consistent with the prediction of a textbook NK model.

This paper highlights the potential benefits and challenges of the RBF estimator in analyses of macroeconomic time series data. The proposed RBF estimator provides a useful starting point for incorporating RBF techniques in macroeconometrics.

8 Appendix

8.1 NK Model for Monte Carlo Simulation

The economy is inhabited by four types of agents: Households, Final good producers, Intermediate goods producers, and Monetary authority. Except for the habit persistence in the household sector, the following NK economy is standard.

8.1.1 Households with Habit Persistence

There is a continuum of households that consume a composite good, C_t, supply labor, N_t, and purchase bond Γ_t. The representative household maximizes the expected lifetime utility given by:

$$E_t \left[\sum_{t=1}^{\infty} \beta^{t-1} \left\{ \frac{(C_t - \gamma C_{t-1})^{1-\sigma}}{1-\sigma} + \frac{(1-N_t)^{1-\kappa}}{1-\kappa} \right\} \right] \tag{15}$$

where γ controls the degree of habit persistence, and β is the discount factor.

The household is subject to the following budget constraint during each period:

$$P_t C_t + \frac{1}{R_t} \Gamma_t = W_t N_t + \Gamma_{t-1} + P_t \Pi_t \tag{16}$$

where $P_t, W_t,$ and R_t are the commodity good price, the nominal wage, and nominal interest rates, respectively. In addition, Π_t is the profit from the intermediate-good firms.

We can maximize the utility subject to the budget constraint to obtain the optimal allocation of consumption across time:

$$\lambda_t = \beta E_t[\lambda_{t+1} R_t / \pi_{t+1}]$$

where $\pi_{t+1} = P_{t+1}/P_t$ and $\lambda_t = (C_t - \gamma C_{t-1})^{-\sigma}$.

The first order condition concerning labor supply decision is

$$W_t = ((1-N_t)^{-\kappa}/\lambda_t)$$

8.1.2 Final Good Producer

There are perfectly competitive final good producers who use intermediate goods, $Y_t(i)$, for $i \in [0,1]$ as inputs and produce final good, Y_t, at a price P_t to maximize the profit given by:

$$\max_{Y_t(i)} P_t Y_t - \int_0^1 P_t(i) Y_t(i) di \tag{17}$$

The technology of the final good producer is given by the following CES aggregator:

$$Y_t = \left(\int_0^1 Y_t(i)^{\frac{(\eta-1)}{\eta}} di \right)^{\frac{\eta}{(\eta-1)}} \tag{18}$$

where $Y_t(i)$ and $P_t(i)$ are quantity and price of an intermediate good i, respectively.

8.1.3 Intermediate Goods Producers

There is a continuum of monopolistically competitive intermediate goods producers who use labor, $N_t(i)$, as an input and solve the following cost minimization problem:

$$\min_{N_t(i)} TC(Y_t(i)) = W_t N_t(i) \tag{19}$$

where TC is nominal total cost. The production technology of the intermediate goods producers are the following:

$$Y_t(i) = A_t N_t(i) \tag{20}$$

where A_t is a productivity shock that follows the AR(1) process given by:

$$\log(A_t) = \rho_a \log(A_{t-1}) + \epsilon_t^a, \quad \epsilon_t^a \backsim N(0, \sigma_a^2) \tag{21}$$

The cost minimization problem of firm i implies

$$mc_t = \frac{W_t}{P_t A_t}$$

where mc_t is the Lagrange multiplier and also the real marginal cost of production.

The intermediate goods producers are subject to Calvo-type price setting friction. In this environment, only a $1 - \upsilon$ fraction of the firms set prices optimally each period: $P_t(i) = P_t^*$,

and the remaining fraction υ of the firms are not allowed to change the price, $P_t(i) = P_{t-1}(i)$. The profit maximization problem of a re-optimizing firm i, which takes into account the probability of adjusting its price next period and onwards, is given by the following:

$$P_t^* \sum_{j=0}^{\infty} \beta^j \upsilon^j E_t \left\{ \Lambda_{t+j} \left[P_t^* Y_{t+j}(i) - P_{t+j} mc_{t+j} Y_{t+j}(i) \right] \right\} \tag{22}$$

where Λ_t is the household's marginal utility of wealth at period t. I assume that the intermediate good producers are owned by the household and that all the profits are transferred to the households. The intermediate goods producers solve the optimization problem described above subject to the demand curve for their own goods, which is given by the following:

$$Y_t(i) = Y_t \left(\frac{P_t(i)}{P_t} \right)^{-\eta} \tag{23}$$

8.1.4 Monetary Authority

Lastly, a monetary authority sets the nominal interest rate according to the Taylor rule as follows:

$$R_t = \max \left[\frac{\bar{\pi}}{\beta} \left(\frac{R_{t-1}}{\bar{\pi}/\beta} \right)^{\phi_R} \left(\left(\frac{\pi_t}{\bar{\pi}} \right)^{\phi_\pi} \left(\frac{Y_t}{\bar{Y}} \right)^{\phi_y} \right)^{1-\phi_R}, 1 \right] \tag{24}$$

where $\bar{\pi}$ is the inflation target, π_t is the inflation rate between $t-1$ and t, and $\bar{Y}$ is the output target. This monetary authority is subject to the zero lower bound, meaning that the monetary authority cannot set the nominal interest rate below zero (or equivalently, $R \geq 1$).

8.1.5 Aggregate Conditions

The aggregate resource constraint is simply given by

$$C_t = Y_t$$

In the Calvo pricing setting, firms that change prices in different periods will have different prices. Therefore, the economy needs to track price dispersion. When firms have different relative prices, there are distortions that create a wedge between the aggregate output measured in terms of production factor inputs and aggregate demand measured in terms of composite goods. Specifically,

$$A_t N_t(i) = Y_t(i) = \left(\frac{P_t(i)}{P_t}\right)^{-\eta} Y_t$$

which implies, in aggregate,

$$N_t = \int_0^1 N_t(i)di = \frac{Y_t}{A_t}\int_0^1 \left(\frac{P_t(i)}{P_t}\right)^{-\eta} di = \frac{Y_t v_t}{A_t}$$

where price dispersion, v_t, can be described as:

$$v_t \equiv \int_0^1 \left(\frac{P_t(i)}{P_t}\right)^{-\eta} di = \upsilon \pi_t^{\eta} v_{t-1} + (1-\upsilon)\left(\frac{P_t^*}{P_t}\right)^{-\eta}$$

8.2 Equilibrium Conditions

I summarize below the first order conditions that characterize the equilibrium of our economy. Let $p_t^* = P_t^*/P_t$ and $a_t = log(A_t)$. Then:

$$\lambda_t = (C_t - \gamma C_{t-1})^{-\sigma} \tag{25}$$

$$\lambda_t = \beta E_t[\lambda_{t+1} R_t/(\pi_{t+1})] \tag{26}$$

$$v_t Y_t = a_t N_t \tag{27}$$

$$mc_t = ((1-N_t)^{-\kappa}/\lambda_t)/a_t \tag{28}$$

$$C_t = Y_t \tag{29}$$

$$R_t = \max\left[\frac{\bar{\pi}}{\beta}\left(\frac{R_{t-1}}{\bar{\pi}/\beta}\right)^{\phi_R}\left(\left(\frac{\pi_t}{\bar{\pi}}\right)^{\phi_\pi}\left(\frac{Y_t}{\bar{Y}}\right)^{\phi_y}\right)^{1-\phi_R}, 1\right] \tag{30}$$

$$p_t^* = ((1-\upsilon\pi^{\eta-1})/(1-\upsilon))^{1/(1-\eta)} \tag{31}$$

$$v_t = \upsilon \pi_t^{\eta} v_{t-1} + (1-\upsilon) p_t^{*-\eta} \tag{32}$$

$$S_t = \lambda_t mc_t Y_t + \beta \upsilon E_t[\pi_{t+1}^{\eta} S_{t+1}] \tag{33}$$

$$F_t = \lambda_t Y_t + \beta \upsilon E_t[\pi_{t+1}^{\eta-1} F_{t+1}] \tag{34}$$

$$p_t^* = S_t/F_t \tag{35}$$

8.3 Numerical Solution of Nonlinear NK Model

The zero lower bound in the Taylor rule introduces the nonlinearity in the NK model. Thus, the solution to the equilibrium condition must be obtained using a global solution method. I use the projection method. Let $S = [v_t, C_{t-1}, R_{t-1}, a_t]$ be the state variables of the model. There are three future variables, $[\pi_{t+1}(S), Y_{t+1}(S), F_{t+1}(S)]$, that need to be interpolated. I approximate each of the future variables with the Radial Basis Functions, $[\pi_{t+1}(\tilde{S}), Y_{t+1}(\tilde{S}), F_{t+1}(\tilde{S})]$, in such a way that equilibrium conditions of the model are satisfied at a set of collocation points, $\tilde{S}$. These collocation points, $\tilde{S}$, are selected using the Maliar and Maliar (2015)'s Epsilon-Distinguishable Set algorithm. The solution's accuracy is presented in the Appendix 8.5. The model is calibrated to a set of standard parameter values in the NK literature. The calibrated parameter values are listed in Appendix 8.4.

The algorithm for the model's numerical solution is given below. There are two loops in the algorithm. The outer loop iterates over the grid, and the inner loop iterates over policy functions.

Step 0a: Solve the log-linear version of the model and simulate data. This initial step is required for the clustering methods in Step 1.

Step 0b: **Define the grid and the polynomials of the RBF**. Given the simulated data, construct a grid following Maliar and Maliar (2015) and estimate the RBF coefficients for the policy functions.

Step 1: **Compute integrals**. Compute the integrals according to Maliar and Maliar (2015)

Step 2: **Equilibrium conditions**. For each grid points, use the polynomials obtained in Step 1 to compute the values of future variables, $[\pi_{t+1}(\tilde{S}), Y_{t+1}(\tilde{S}), F_{t+1}(\tilde{S})]$. Given the future variables, solve for the endogenous state variables next period using the model's equilibrium conditions.

Step 3: **Evaluate conditional expectations**. Using the integrals computed in Step 1, evaluate the conditional expectations in equations 27, 33, 34.

Step 4: **Evaluate new policy functions**. Given the conditional expectations, obtain new values of future variables in the current period, $[\pi'_t(\tilde{S}), Y'_t(\tilde{S}), F'_t(\tilde{S})]$, using equations 27, 33, 34. Given these new values, compute the new policy functions, and compute the

difference between the polynomials of newly obtained policy functions and those of old policy functions. Denote the percentage difference as r.

Step 5: **Iteration**. If $r < 10^{-8}$, go to Step 6. Otherwise, update the guess and repeat Step 1-5.

Step 6: **Compute new grid**. Using the solution obtained in the previous steps, simulate new data. Using these simulated data, choose a new grid using Maliar and Maliar (2015). Compute the difference between the old grid and the new grid. Specifically, for each newly computed grid point, find the nearest point in the old grid and compute the Euclidean distance. This forms a vector, D, that contains the distances between each new grid point to its nearest point in the old grid. Find the maximum of D and call it r_g.

Step 7: **Iteration for grid**. If r_g is smaller than the Euclidean distance between the farthest two points in the old grid, stop the algorithm. Otherwise, go back to Step 2 with the new grid obtained in Step 6.

8.4 Calibration

The parameter values for calibration of the New Keynesian model are summarized in Table 3.

Table 3: Calibration

parameter	value	description
γ	0.5	Habit Persistence
β	0.99	Discount factor
σ	1	Utility Curvature: Consumption
κ	2.65	Utility Curvature: Leisure
υ	0.60	Calvo: $(1-\upsilon)\%$ adjust prices each period
η	9	Price Elasticity of Demand
$\bar{\pi}$	1	Inflation Target
ϕ_π	2.21	Taylor Rule inflation coefficient
ϕ_y	0.07	Taylor Rule output gap coefficient
ϕ_R	0.82	Interest Rate Smoothing
ρ_a	0.80	Prod. shock persistence
σ_a	0.019	Prod. shock std.

8.5 Accuracy of Numerical Solution

I check the accuracy of the numerical solution by computing the errors of the residual equations. Specifically, I proceed as follows. First, I simulate the model forward for 10,000 periods. This gives a simulation for both the state and control variables of the model for 10,000 periods. Second, compute the residuals from the intertemporal equations 27, 33, 34 for the 10,000 periods. I report the decimal log of the absolute value of these residual errors.

On average, residual equation errors are on order of -3.53 for equation 27, -4.94 for equation 33, and -2.58 for equation 34. These numbers are comparable to those established by other studies whose models have similar degrees of complexity.

Figure 8: Residual equation errors

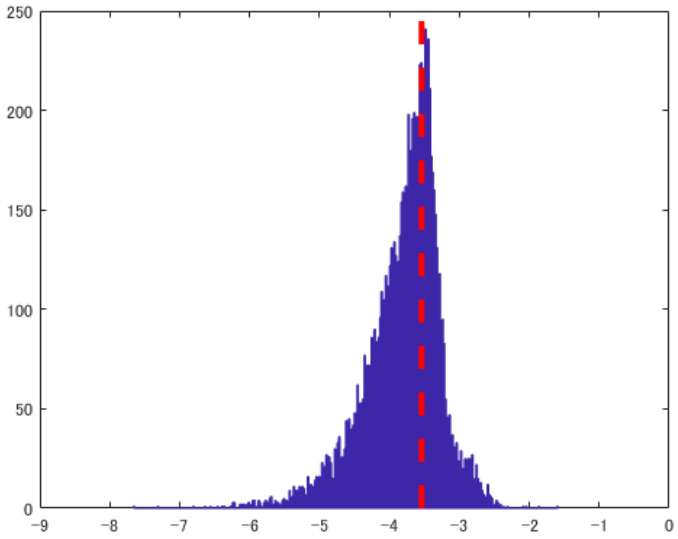

(a) Equation 27

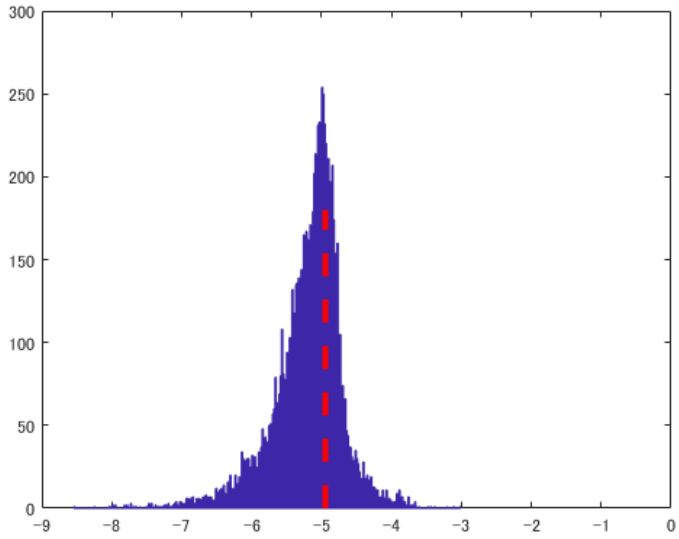

(b) Equation 33

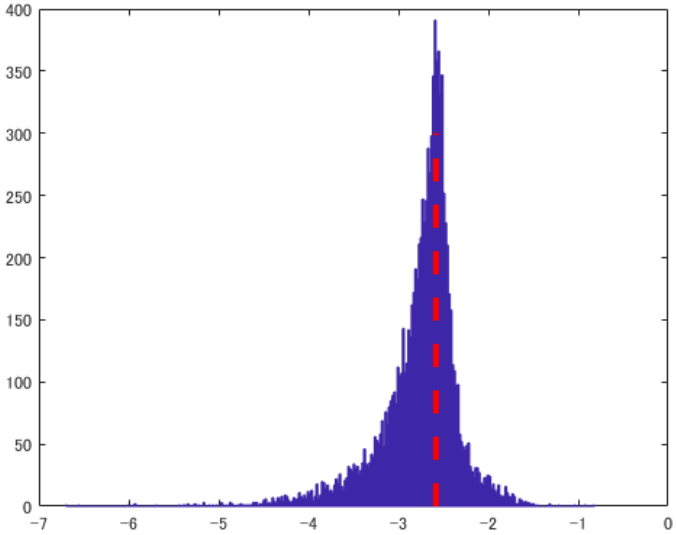

(c) Equation 34

Notes: The histograms report the residual equation errors in decimal log basis. The dotted red lines mark the mean residual equation errors.

8.6 Threshold VAR Estimation

To estimate Equation 9, I impose a natural conjugate prior on the VAR parameters by adding the following dummy observation as suggested by Sims and Zha (1998) and Bańbura, Giannone, and Reichlin (2010):

$$\mathbf{Y}_{D,1} = \begin{pmatrix} diag(\gamma_1\sigma_1, \dots \gamma_K\sigma_K)/\tau \\ 0_{K\times(P-1)\times K} \\ \cdots\cdots\cdots\cdots \\ diag(\sigma_1, \dots, \sigma_K) \\ \cdots\cdots\cdots\cdots \\ 0_{1\times K} \end{pmatrix}, \text{ and } \mathbf{X}_{D,1} = \begin{pmatrix} J_p \otimes diag(\sigma_1, \dots, \sigma_K)/\tau & 0_{NP\times 1} \\ \cdots\cdots\cdots\cdots & \\ 0_{K\times KP} & 0_{K\times 1} \\ \cdots\cdots\cdots\cdots & \\ 0_{1\times KP} & c \end{pmatrix} \quad (36)$$

where γ_1 to γ_K denotes the prior mean for the coefficients on the first lag, τ controls the tightness of the prior on the VAR coefficients, c controls the tightness of the prior on the constant terms, and $J_p = diag(1, 2, \dots, P)$. Th prior means are set to the estimated AR(1) regression coefficients, which is estimated for each endogenous variable. The standard deviation of the error terms from these AR(1) regressions are used for the scaling factors σ_i. τ is set to 100, and c is 1/10000, which essentially is equivalent to a flat prior on the constant. I also introduce a prior on the sum of the lagged dependent variables by adding the following dummy observations:

$$\mathbf{Y}_{D,2} = \frac{diag(\gamma_1, \mu_1, \dots \gamma_K\mu_K)}{\lambda}, \text{ and } \mathbf{X}_{D,2} = \begin{pmatrix} \frac{(1_{1\times P})\otimes diag(\gamma_1\mu_1,\dots,\gamma_K\mu_K)}{\lambda} & 0_{K\times 1} \end{pmatrix} \quad (37)$$

where μ_i is the sample averages of the endogenous variables from the training sample. As in Bańbura, Giannone, and Reichlin (2010), the tightness of this sum of coefficients prior is set to $\lambda = 10\tau$. Given the natural conjugate prior, the conditional posterior distributions of the VAR parameters $\Gamma_j = vec(c_j, \Gamma_{j,1}; \Gamma_{j,2}; \dots; \Gamma_{j,P})$ and Ω_j for $j = \{0, 1\}$ are given by:

$$G(\Gamma_j|\Omega_j) \sim N(\Gamma*_j, \Omega_j \otimes (\mathbf{X}*' \mathbf{X}*)^{-1}) \quad (38)$$

$$G(\Omega_j|\Gamma_j) \sim IW(S*_j, T*_j). \quad \text{for } j = \{0, 1\} \tag{39}$$

For $j = \{0, 1\}$, the posterior means are defined by $\Gamma*_j = (\mathbf{X} *'_j \mathbf{X}*_j)^{-1}(\mathbf{X} *'_j \mathbf{Y}*_j)$ and $S*_j = (\mathbf{Y} *_j - \mathbf{X} *_j \tilde{\Gamma}_j)'(\mathbf{Y} *_j - \mathbf{X} *_j \tilde{\Gamma}_j)$, where $\mathbf{Y}*_j = [\mathbf{Y}_j; \mathbf{Y}_{D,1}; \mathbf{Y}_{D_2}]$, $\mathbf{X}* = [\mathbf{X}_j; \mathbf{X}_{D,1}; \mathbf{X}_{D_2}]$ and $\tilde{\Gamma}_j$ is the draw of the VAR coefficients Γ_j rearranged to be consistent with $\mathbf{X}*_j$. $T*_h$ is the number of rows of $\mathbf{Y}*_j$.

By drawing successively from these conditional posteriors, I use the Gibbs sampler to simulate the posterior distribution of Γ_j and Ω_j. I use 20,000 iterations with the last 5000 used to produce the forecast density given by:

$$G(\mathbf{Y}_{t+h}|\mathbf{Y}_t) = \int G(\mathbf{Y}_{t+h}|\mathbf{Y}_t, \Gamma) \times G(\Gamma|\mathbf{Y}_t) d\Gamma \tag{40}$$

where $h = 1, 2, 3, 4$ and $\Gamma = \{\Gamma_1, \Omega_1, \Gamma_0, \Omega_0, R*, d\}$. To estimate d and $R*$, I assume a flat prior on d and restrict its maximum value to four. I assume a normal prior for $R* \sim N(\tilde{R}, \tilde{\nu})$, where $\tilde{R} = 1/T \sum_{i=1}^{T} R_t$ and $\tilde{\nu} = 10$. I employ the Gibbs sampler introduced in Chen and Lee (1995) to simulate the posterior distribution of the unknown parameters. Given an initial value for $R*$ and d, the conditional posterior for the VAR parameters in the two regimes is determined by equations 38 and 39. Given a draw for the VAR parameters and a value for d, a random walk Metropolis Hastings step is used to sample $R*$. We draw candidate value of $R*_{\text{new}}$ from $R*_{\text{new}} = R *_{\text{old}} + \Psi^{1/2}\epsilon$, $\epsilon \sim N(0, 1)$. The acceptance probability is given by $g(\mathbf{Y}_t|R*_{\text{new}}, \Psi)/g(\mathbf{Y}_t|R*_{\text{old}}, \Psi)$ where $g(\cdot)$ denotes the posterior density and Ψ represents all other parameters in the model. Chen and Lee (1995) show that the conditional posterior for d is a multinomial distribution with probability, $L(\mathbf{Y}_t|d, \Psi)/\sum_{d=1}^{4} L(\mathbf{Y}_t|d, \Psi)$, where $L(\cdot)$ is the likelihood function. The forecast density can be computed by iterating equations 9 and 10 forward using the Gibbs draws for $\Gamma's$ and $\Omega's$.

8.7 Examples of the RBF Generalized Impulse Responses

Examples of the generalized impulse responses are illustrated in Figure 9. For this illustration, I selected a sample of 300 consecutive periods from the simulated data and estimated the VAR(4) and RBF(1).[21] To draw impulse responses, I pick two random histories, ω_{t-1},

[21] VAR(4) denotes the VAR model with 4 lags, and RBF(1) means the RBF estimator with 1 lag.

from the sample and ensure that one of the selected histories satisfies the criterion for the normal state while the other satisfies the criterion for the zlb state. I then calculate the impulse responses with the shock occurring at these two histories.

In Figure 9, the blue solid line shows the *true* impulse response under the normal state, while the red solid line shows the *true* impulse response under the zlb state. In addition to the true impulse responses, the left panels show the estimated responses from the RBF(1) estimator under the normal state in the blue dotted line and under the zlb state in the red dotted line. Shaded bands represent the 2.5th and 97.5th percentiles.[22] The right panels show the estimated impulse responses from the linear VAR(4) with 95 percent confidence bands in black lines.

The top panels of Figure 9 show the responses of the inflation rate following a positive productivity shock. The positive productivity shock is deflationary. The figure shows that the initial impact of the shock is slightly larger in magnitude during the normal state, which reduces the inflation rate by 0.7% on impact. The inflation rate under the normal state then quickly returns to zero after three periods. The decline of the inflation rate is smaller under the zlb. The inflation rate goes down by 0.42% on impact, and the response is slightly more persistent under the zlb. The RBF(1) estimator appears to successfully capture the different responses of the inflation rate under the two different states. Moreover, the confidence bands are reasonably narrow even when they are compared to those of the linear VAR(4) model. As expected, the linear VAR(4) only captures the response during the normal state.

The next panels in Figure 9 show the responses of the interest rate. When the positive productivity shock creates a deflationary pressure in the economy, the central bank follows the Taylor rule by lowering the nominal interest rate during the normal state. The response of the interest rate is smaller during the zlb periods because the central bank is unable to push down the interest rate any further.[23] The left panel shows that the RBF(1) estimator once again successfully capture the different interest rate responses under the two different

[22]The confidence bands are estimated by the residual-based block bootstrap method. When I conduct the bootstrap, the centroids and scaling parameters are re-estimated by repeating the K-means cluster method for 50 times with different initial values and by selecting the centroids that minimize the errors. My baseline preference is block bootstrap method rather than the wild bootstrap because the residuals exhibit auto-correlation. The results are almost identical when the wild bootstrap is employed.

[23]The nominal interest rates appears to go down in the figure, but the responses shown here are *relative* to the counterfactual where the shock did not occur. Thus, the negative interest rates response during the zlb state actually indicate that the interest rates would have increased from zero faster if the shock did not arrive. (If the shock did not occur, interest rate rises from zero whereas if the shock occurs, the interest rate stayed zero. The difference between the shock scenario and non-shock scenario is negative.)

regimes. Furthermore, the RBF(1) estimator can distinguish in a statistically significant manner the two different interest rate responses under the zlb state and normal state.

Finally, Figure 10 shows the responses of consumption. Due to the positive productivity shock, the consumption goes up in both normal and zlb states. The consumption responses peak during the third quarter, reaching 1.2% in the normal state and 1% in the zlb state. The weak response during the zlb periods stems from the higher real interest rate, which is caused by the absence of the central bank's reaction to the deflationary pressure. As the real interest rate goes up during the zlb periods, the consumption is discouraged. The RBF(1) estimator seems to reasonably capture the different consumption dynamics that follow the positive supply shock. In addition, the responses under the two regimes can be distinguished in a statistically significant manner.

Figure 9: Examples of Generalized Impulse Responses

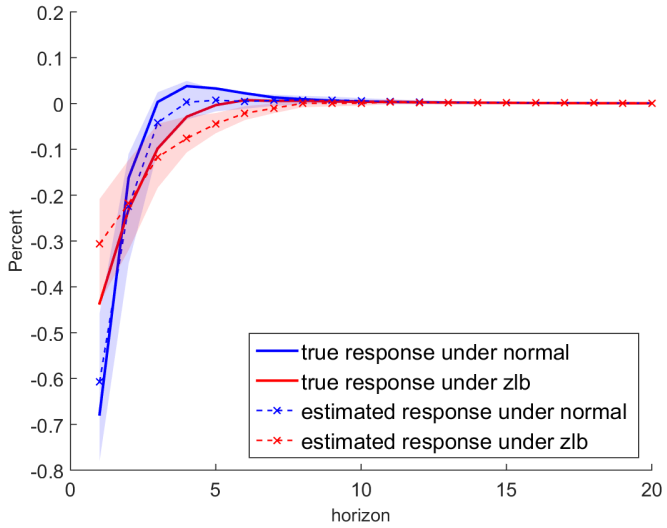

Inflation: RBF(1)

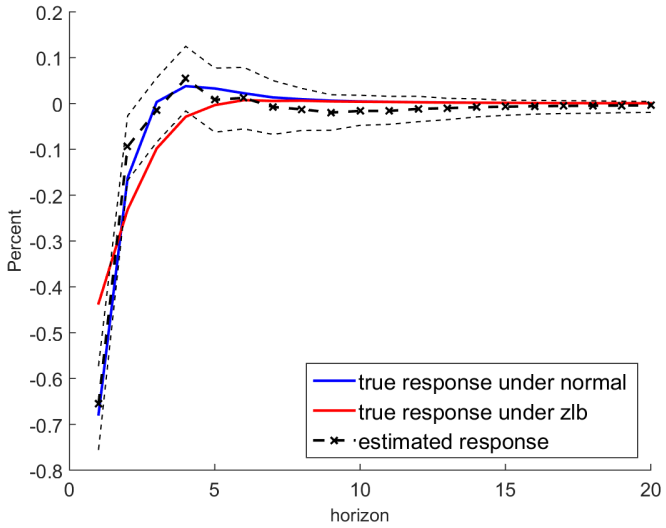

Inflation: VAR(4)

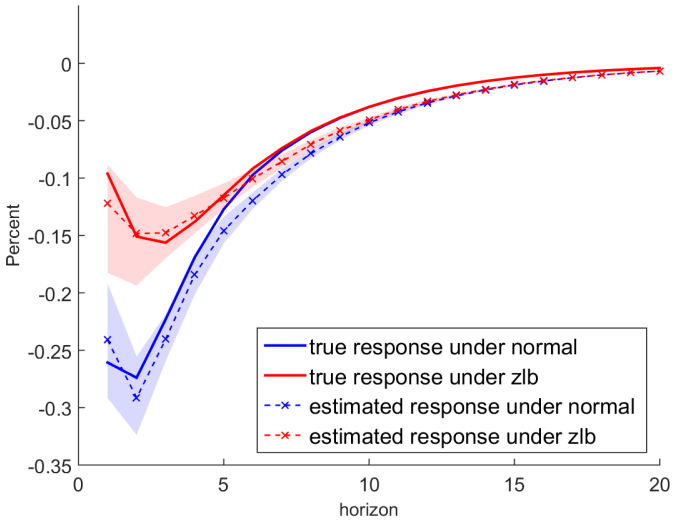

Interest Rate: RBF(1)

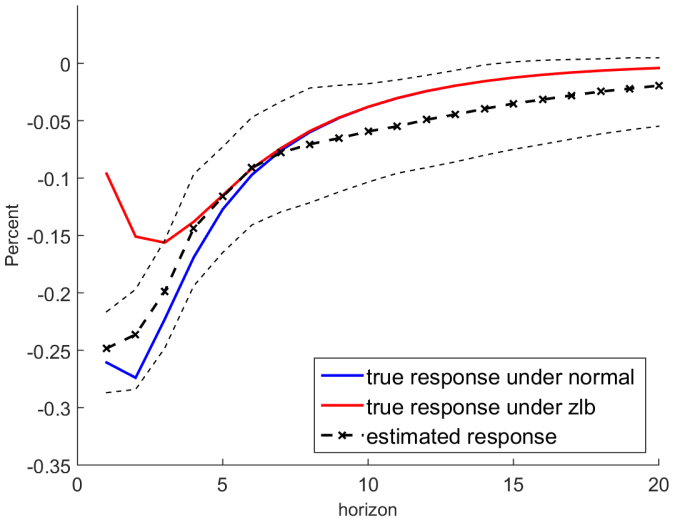

Interest Rate: VAR(4)

Figure 10: Examples of Generalized Impulse Responses

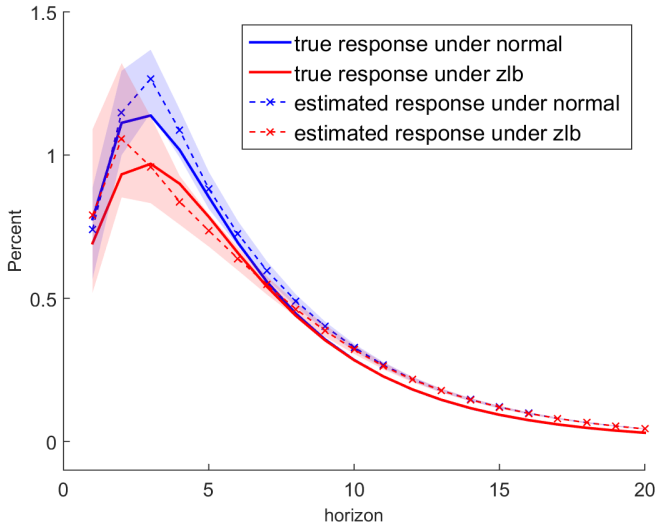

Consumption: RBF(1)

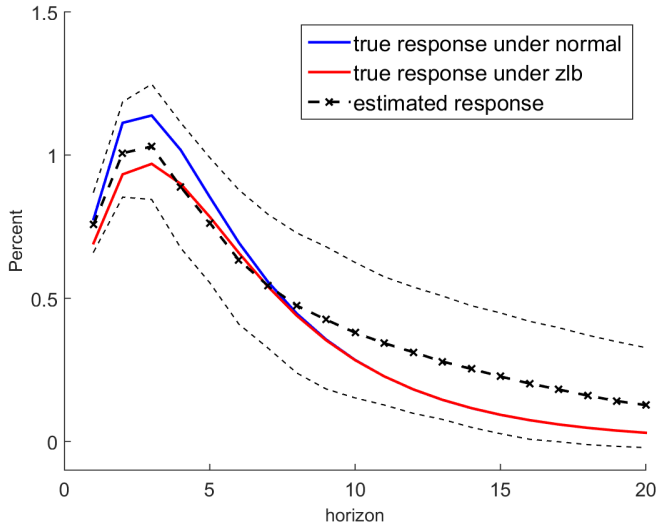

Consumption: VAR(4)

Notes: Impulse response functions of the inflation rate, interest rate, and consumption (in percent) to a one standard-deviation positive productivity shock. True structural impulse responses from the NK model in the normal state (blue solid line) or the zlb state (red solid line). Estimation from a RBF(1) in the normal state (blue dashed line) or the zlb state (red dashed line). Estimated impulse response from a VAR(4) (black dashed line). Shaded bands denote the 2.5th and 97.5th percentiles estimated by the residual-based block bootstrap method.

8.8 Additional Figures

Figure 11: Federal funds rate

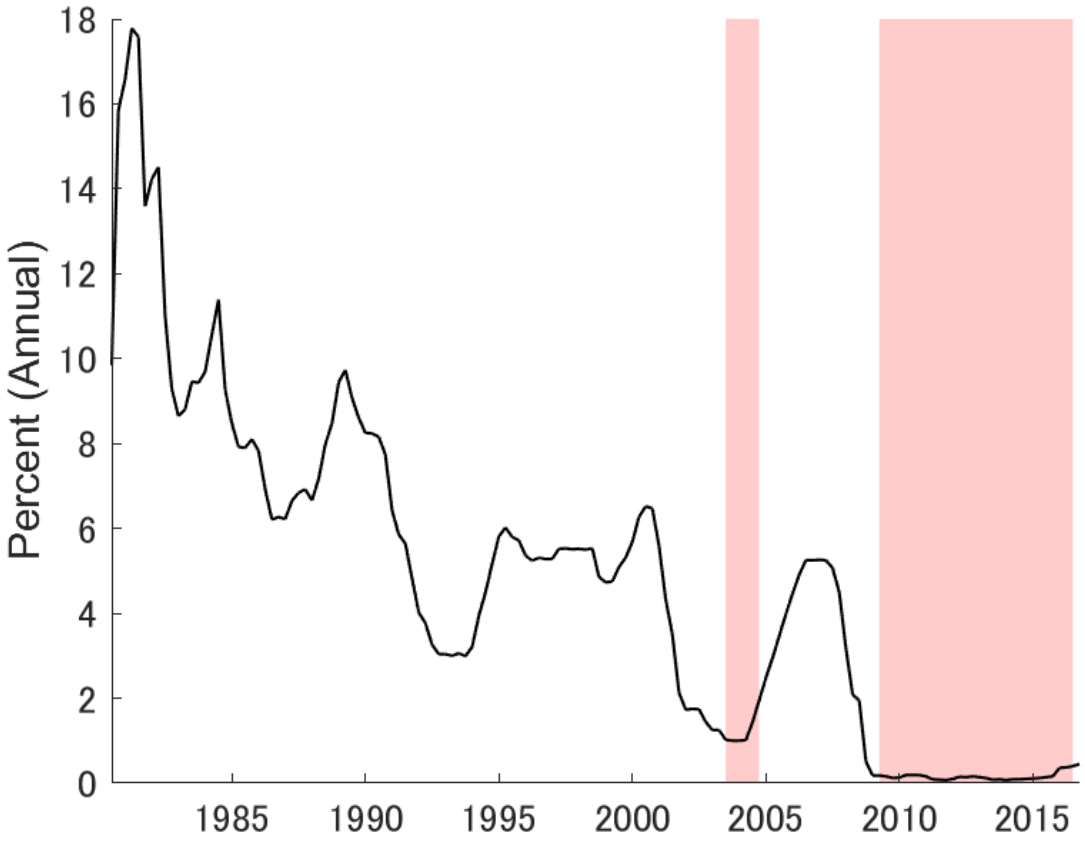

Notes: Federal funds rate between 1980 and 2016. Red shaded areas represent the periods of weak output responses outside the recession dates.

Figure 12: Responses of cumulative GDP

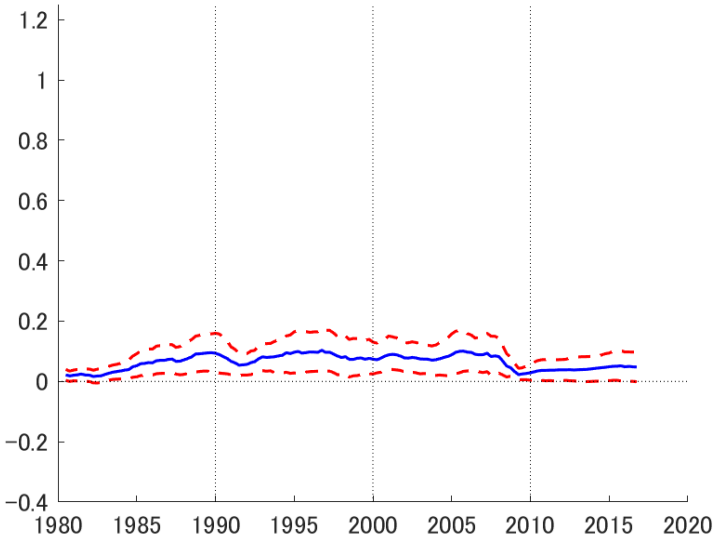

(a) Response after 1st quarter

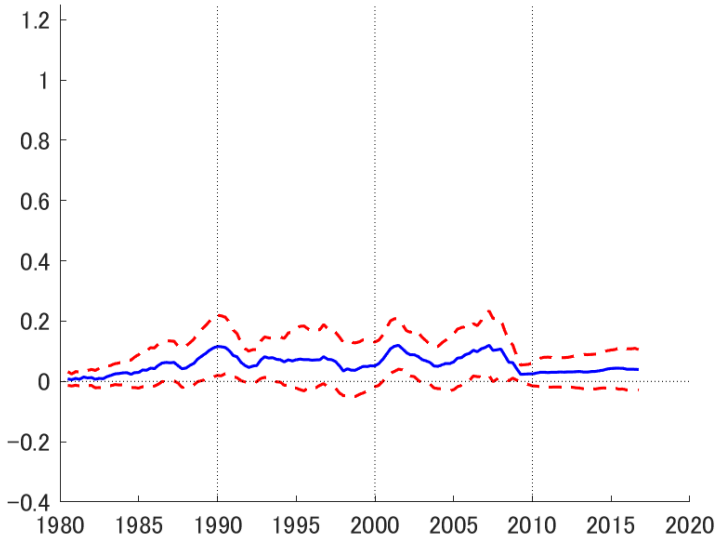

(b) Response after 2nd quarter

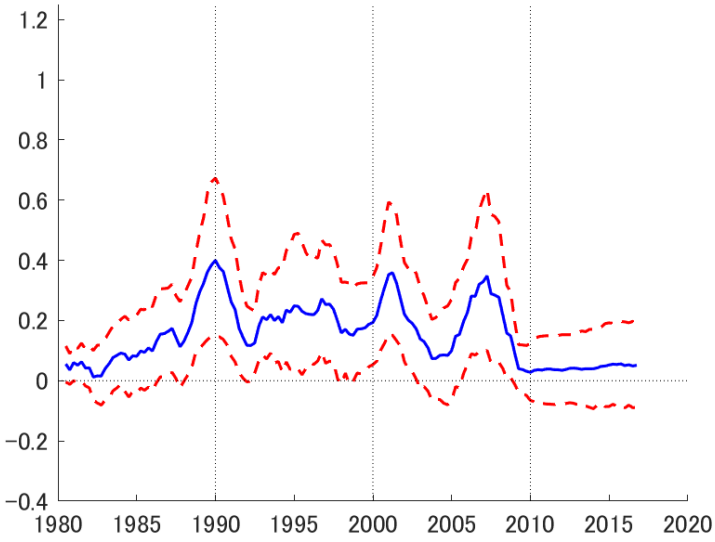

(c) Response after 5th quarter

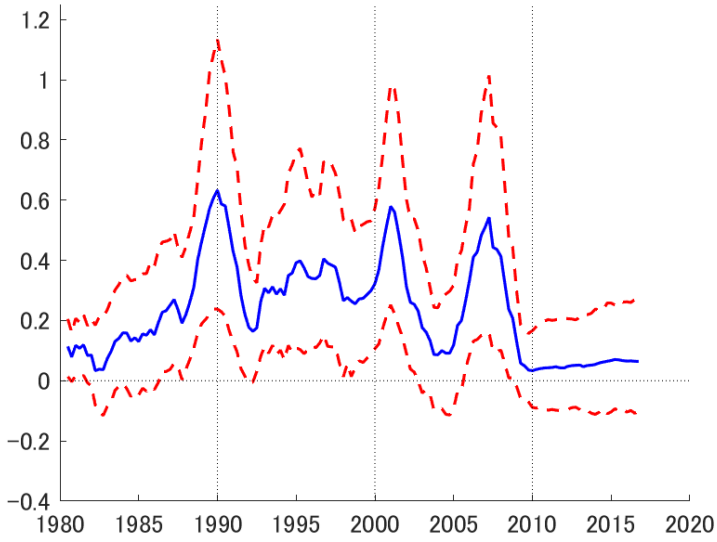

(d) Response after 9th quarter

Notes: Impulse response functions of the cumulative real GDP (in percent) to a one standard-deviation positive TFP shock. Shaded bands denote the 68% confidence interval estimated by the residual-based block bootstrap method.

Figure 13: Responses of Expected Inflation

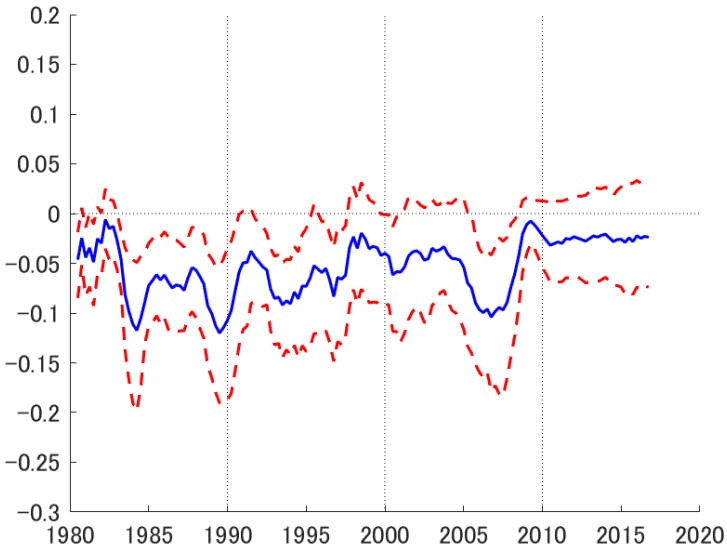

(a) Response after 1st quarter

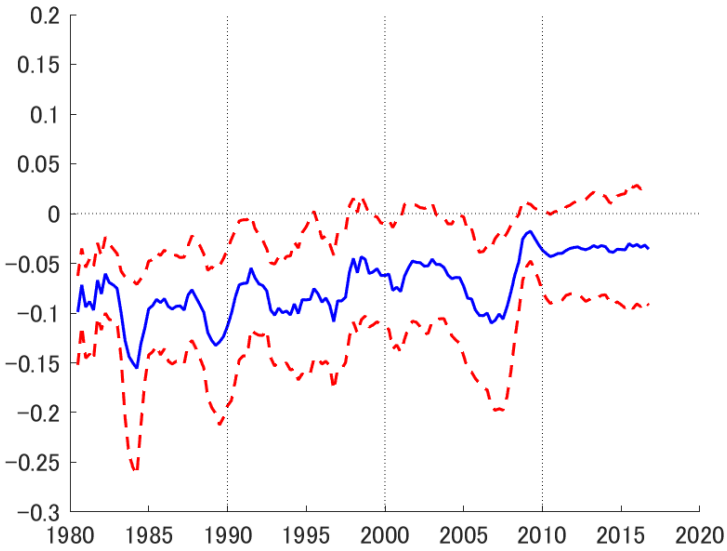

(b) Response after 2nd quarter

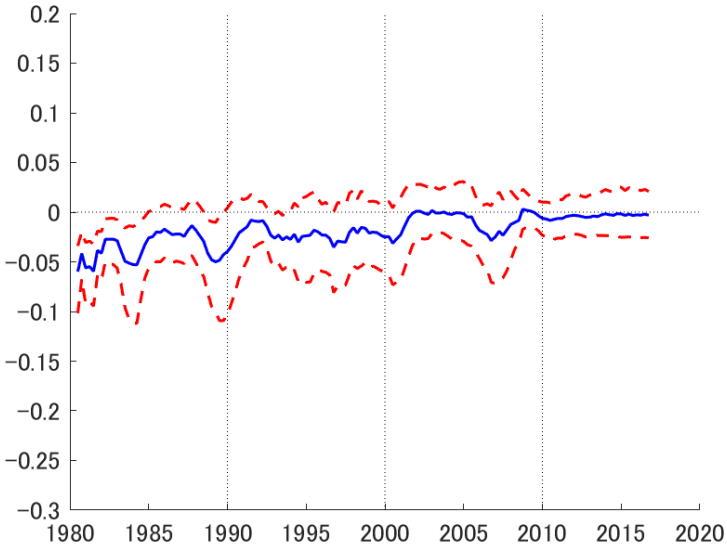

(c) Response after 5th quarter

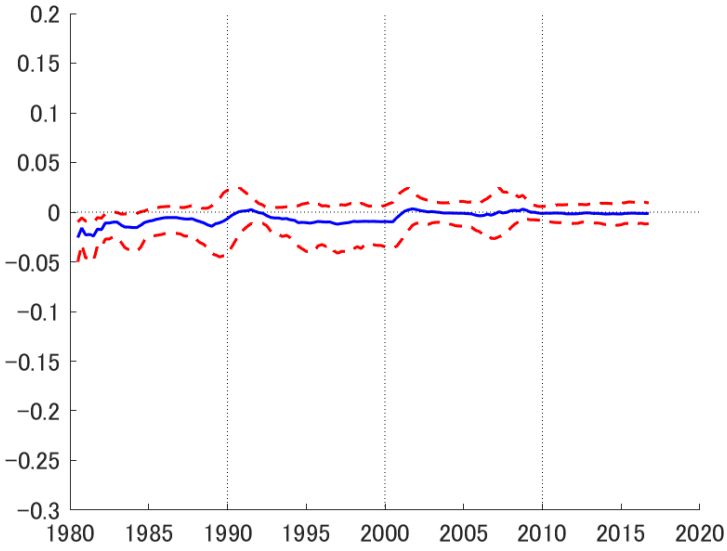

(d) Response after 9th quarter

Notes: Impulse response functions of the expected inflation (in percent) to a one standard-deviation positive TFP shock. Dotted lines show the 68% confidence bands estimated by the residual-based block bootstrap method.

Figure 14: Responses of Fed Funds rate

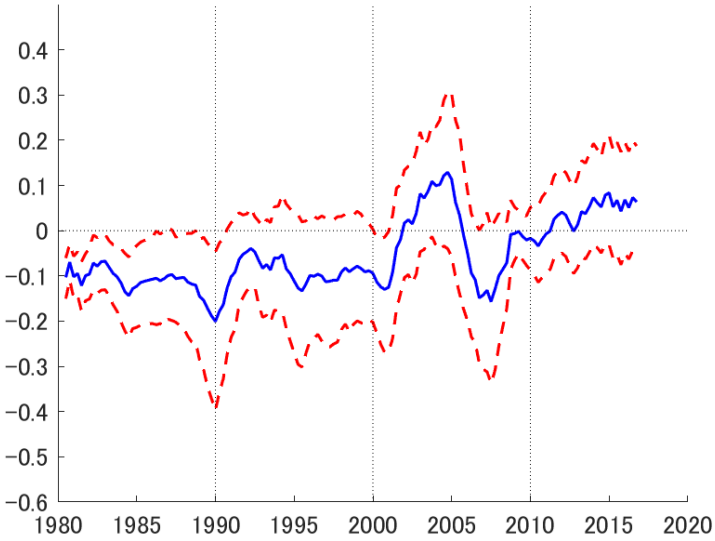

(a) Response after 1st quarter

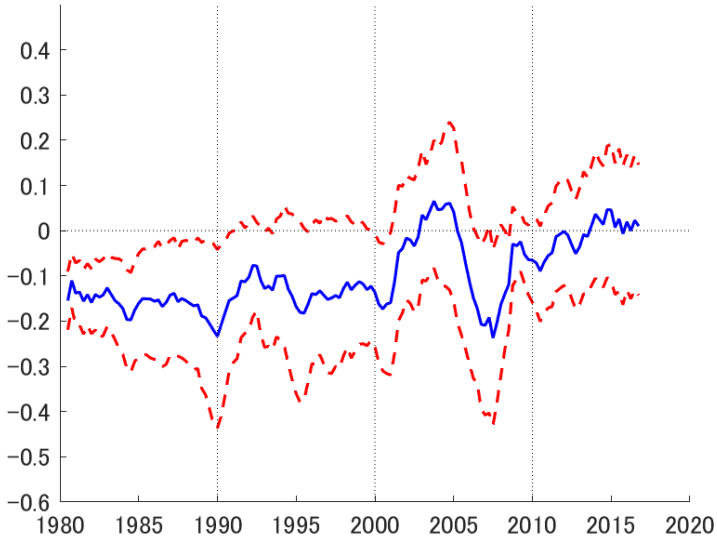

(b) Response after 2nd quarter

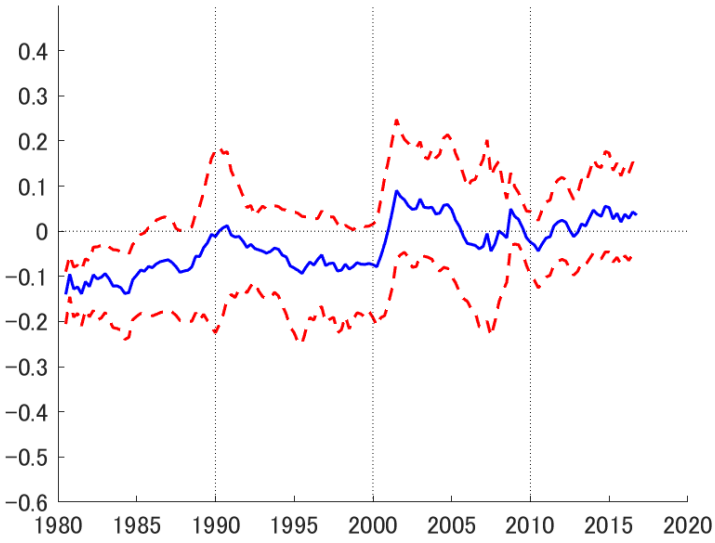

(c) Response after 5th quarter

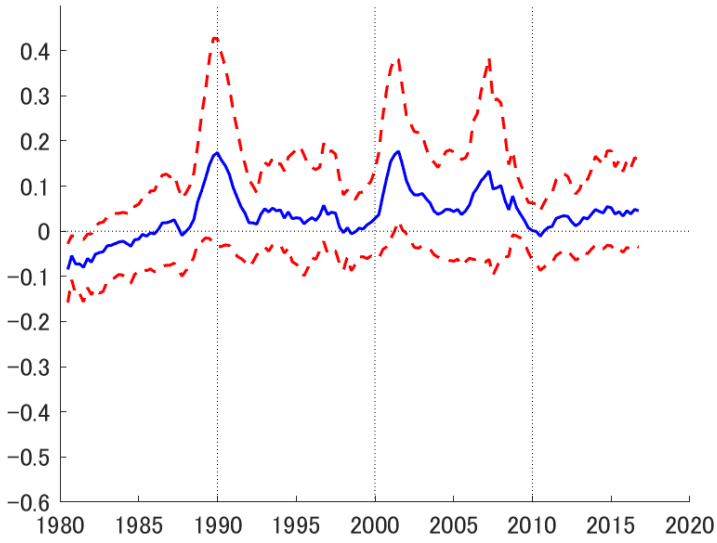

(d) Response after 9th quarter

Notes: Impulse response functions of the fed funds rate (in percent) to a one standard-deviation positive TFP shock. Dotted lines show the 68% confidence bands estimated by the residual-based block bootstrap method.

Figure 15: Responses of real interest rate

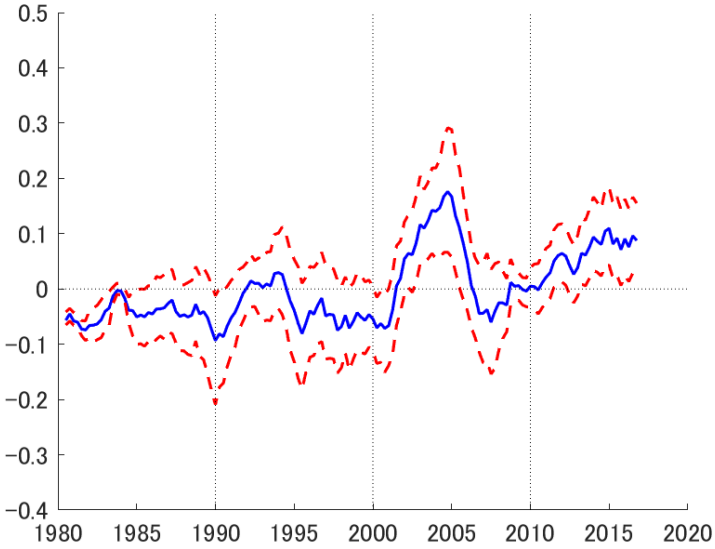

(a) Response after 1st quarter

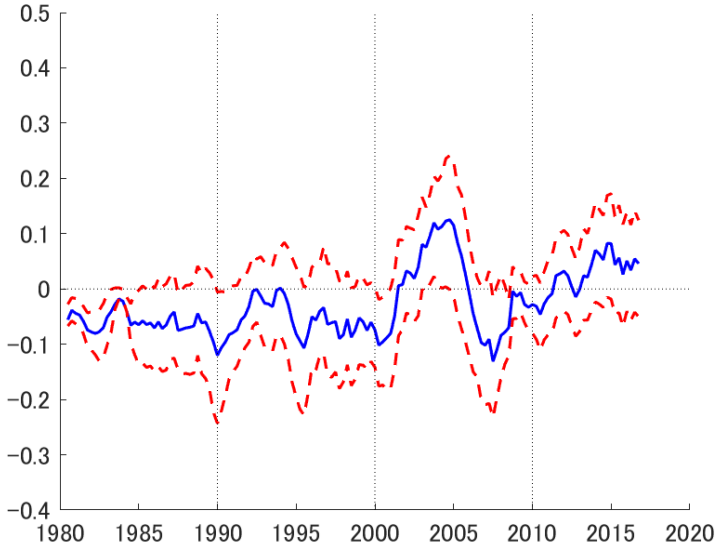

(b) Response after 2nd quarter

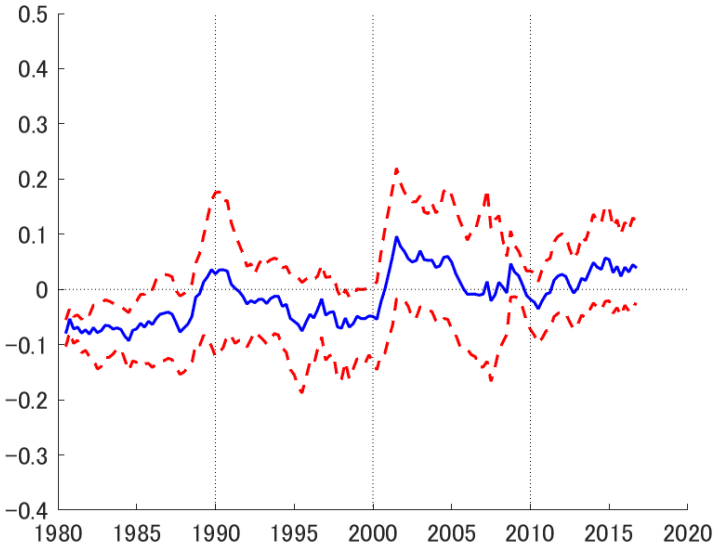

(c) Response after 5th quarter

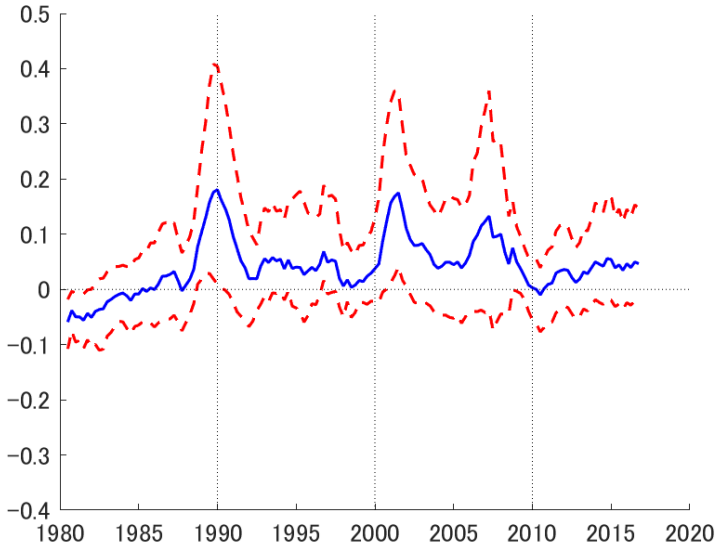

(d) Response after 9th quarter

Notes: Impulse response functions of real interest rate (in percent) to a one standard-deviation positive TFP shock. Dotted lines show the 68% confidence bands estimated by the residual-based block bootstrap method.

Figure 16: Responses of cumulative Consumption

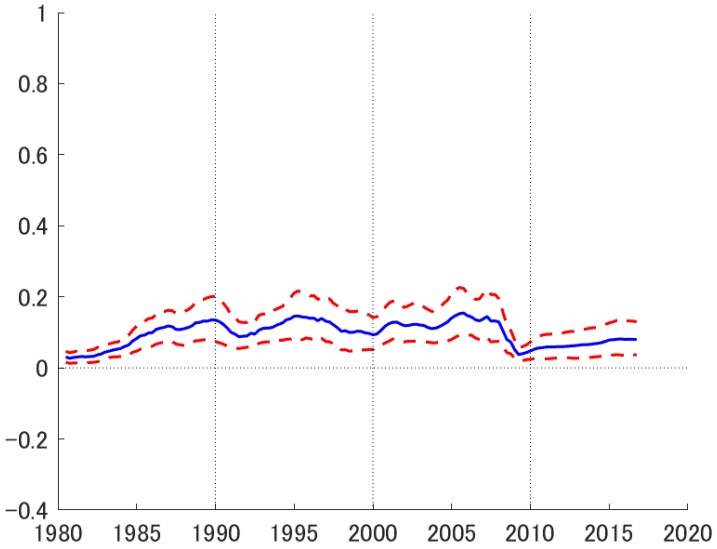

(a) Response after 1st quarter

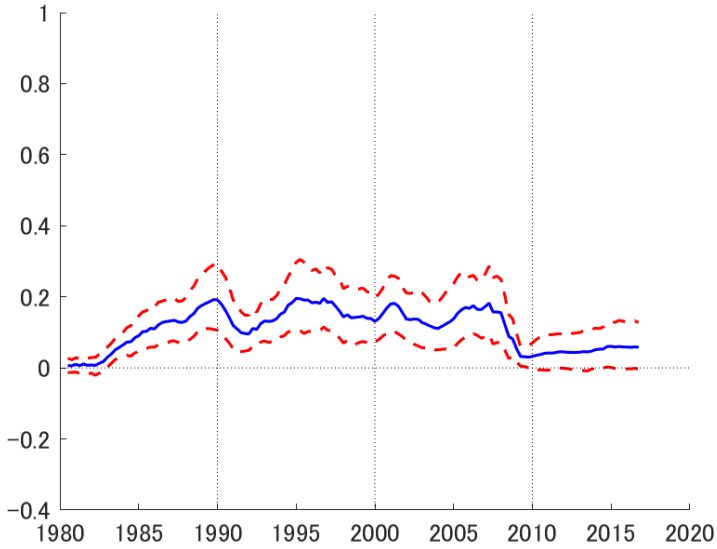

(b) Response after 2nd quarter

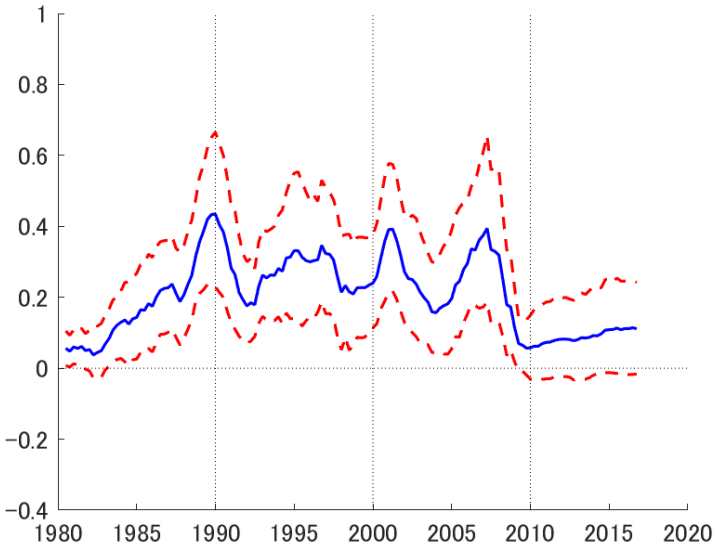

(c) Response after 5th quarter

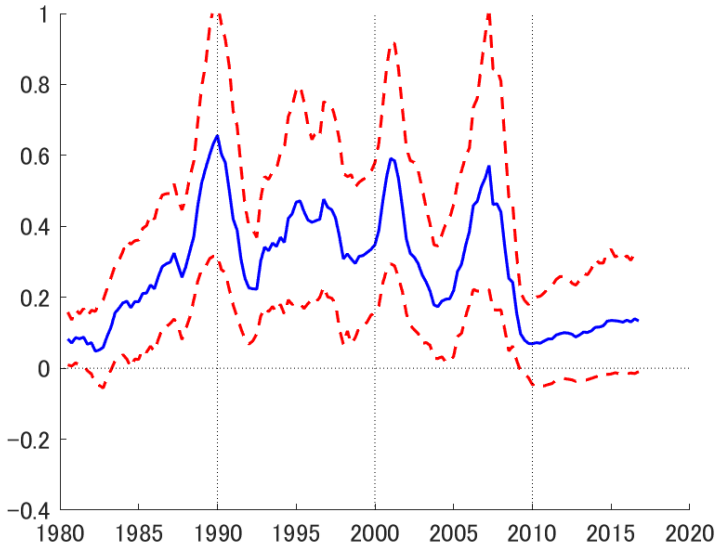

(d) Response after 9th quarter

Notes: Impulse response functions of consumption (in percent) to a one standard-deviation positive TFP shock. Dotted lines show the 68% confidence bands estimated by the residual-based block bootstrap method.

Figure 17: Responses of Hours Worked

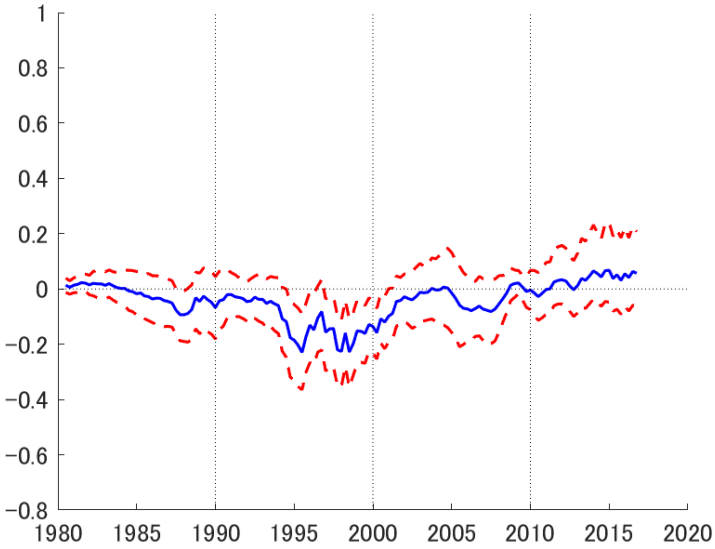

(a) Response after 1st quarter

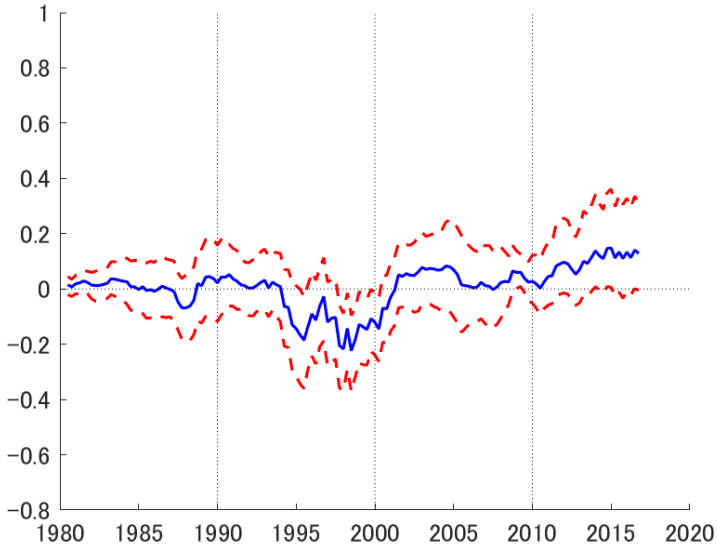

(b) Response after 2nd quarter

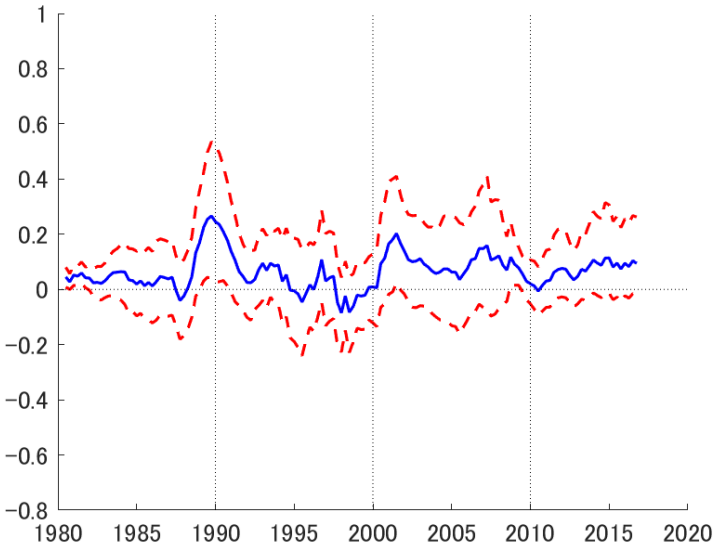

(c) Response after 5th quarter

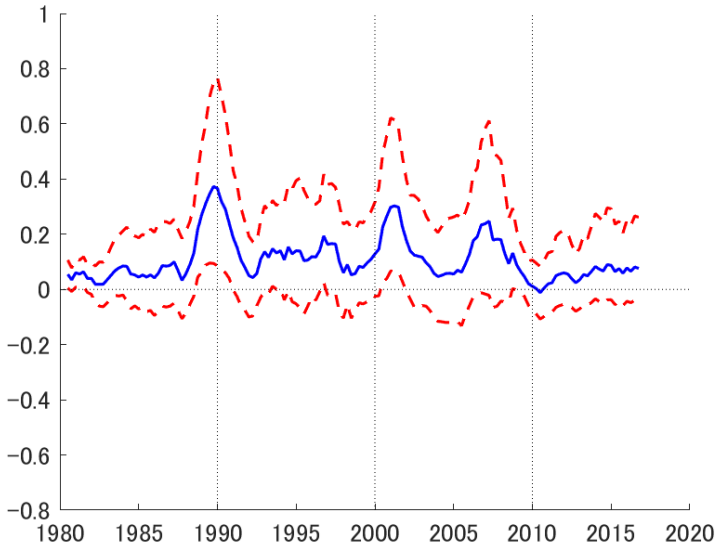

(d) Response after 9th quarter

Notes: Impulse response functions of hours worked (in percent) to a one standard-deviation positive TFP shock. Dotted lines show the 68% confidence bands estimated by the residual-based block bootstrap method.

Figure 18: Responses of cumulative Investment

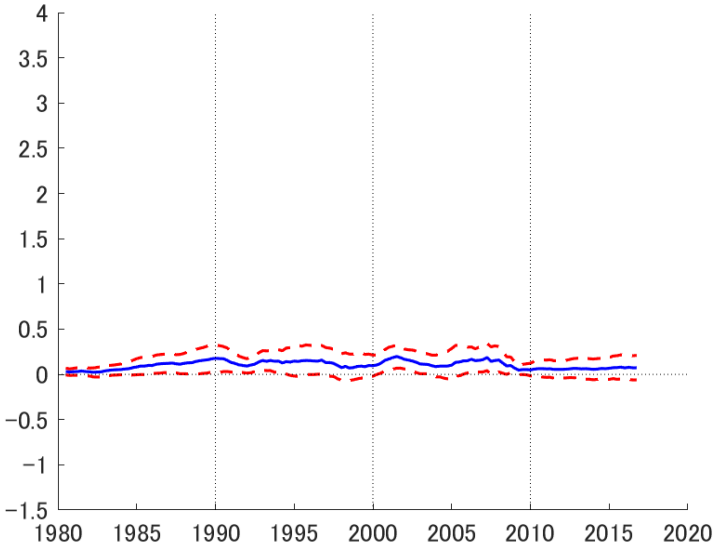

(a) Response after 1st quarter

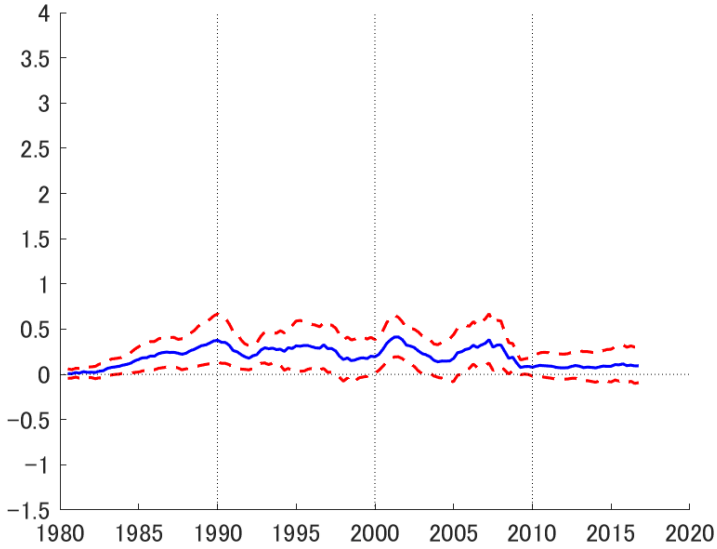

(b) Response after 2nd quarter

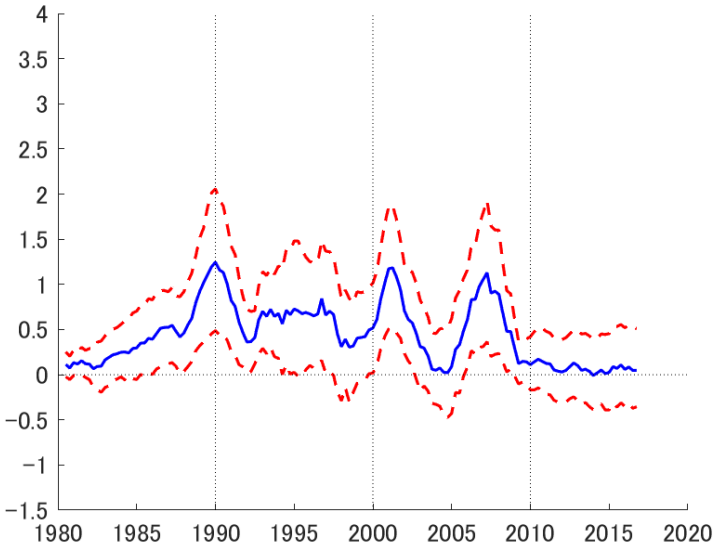

(c) Response after 5th quarter

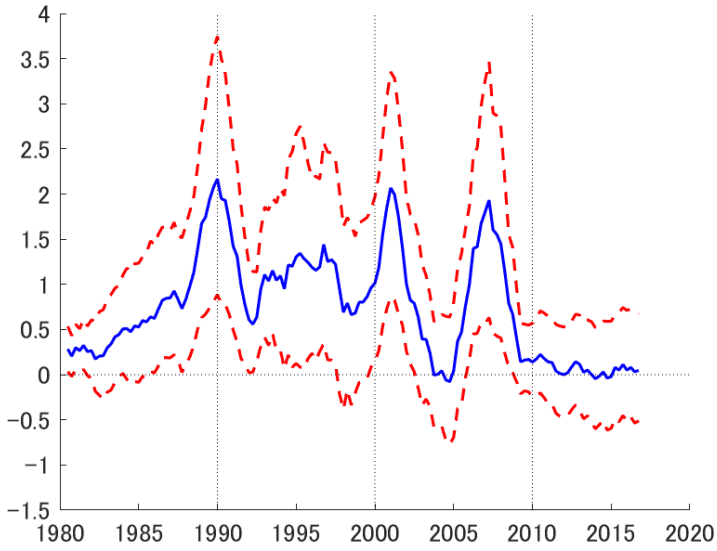

(d) Response after 9th quarter

Notes: Impulse response functions of investment (in percent) to a one standard-deviation positive TFP shock. Dotted lines show the 68% confidence bands estimated by the residual-based block bootstrap method.

References

Alessandri, P. and H. Mumtaz (2017). Financial conditions and density forecasts for us output and inflation. *Review of Economic Dynamics 24*, 66–78.

Balke, N. S. and T. B. Fomby (1997). Threshold cointegration. *International Economic Review*, 627–645.

Bańbura, M., D. Giannone, and L. Reichlin (2010). Large bayesian vector auto regressions. *Journal of Applied Econometrics 25*(1), 71–92.

Barnichon, R. and C. Matthes (2018). Functional approximation of impulse responses. *Journal of Monetary Economics 99*, 41–55.

Beaudry, P. and G. Koop (1993). Do recessions permanently change output? *Journal of Monetary Economics 31*(2), 149–163.

Blake, A. P. and G. Kapetanios (2000). A radial basis function artificial neural network test for arch. *Economics Letters 69*(1), 15–23.

Blake, A. P. and G. Kapetanios (2003). A radial basis function artificial neural network test for neglected nonlinearity. *The Econometrics Journal 6*(2), 357–373.

Blake, A. P. and G. Kapetanios (2007a). Testing for arch in the presence of nonlinearity of unknown form in the conditional mean. *Journal of Econometrics 137*(2), 472–488.

Blake, A. P. and G. Kapetanios (2007b). Testing for neglected nonlinearity in cointegrating relationships. *Journal of Time Series Analysis 28*(6), 807–826.

Broomhead, D. S. and D. Lowe (1988). Radial basis functions, multi-variable functional interpolation and adaptive networks. *Complex System 2*, 321–355.

Camacho, M. (2004). Vector smooth transition regression models for us gdp and the composite index of leading indicators. *Journal of Forecasting 23*(3), 173–196.

Canova, F. (1993). Modelling and forecasting exchange rates with a bayesian time-varying coefficient model. *Journal of Economic Dynamics and Control 17*(1-2), 233–261.

Canova, F. and L. Gambetti (2009). Structural changes in the us economy: Is there a role for monetary policy? *Journal of Economic Dynamics and Control 33*(2), 477–490.

Chan, J. C., E. Eisenstat, and R. W. Strachan (2020). Reducing the state space dimension in a large tvp-var. *Journal of Econometrics*.

Chen, C. W. and J. C. Lee (1995). Bayesian inference of threshold autoregressive models. *Journal of Time Series Analysis 16*(5), 483–492.

Chen, S., C. F. Cowan, and P. M. Grant (1991). Orthogonal least squares learning algorithm for radial basis function networks. *IEEE Transactions on Neural Networks 2*(2), 302–309.

Cogley, T. and T. J. Sargent (2001). Evolving post-world war ii us inflation dynamics. *NBER Macroeconomics Annual 16*, 331–373.

Cogley, T. and T. J. Sargent (2005). Drifts and volatilities: monetary policies and outcomes in the post wwii us. *Review of Economic Dynamics 8*(2), 262–302.

Fernald, J. G. (2014). A quarterly, utilization-adjusted series on total factor productivity. Federal Reserve Bank of San Francisco.

Fernández-Villaverde, J., S. Hurtado, and G. Nuno (2018). Financial frictions and the wealth distribution. *Manuscript, University of Pennsylvania*.

Friedman, J., T. Hastie, and R. Tibshirani (2008). *The Elements of Statistical Learning* (Second ed.). Springer Series in Statistics New York.

Gallant, A. R. and G. Tauchen (1989). Seminonparametric estimation of conditionally constrained heterogeneous processes: Asset pricing applications. *Econometrica*, 1091–1120.

Galvao, A. B. and M. Marcellino (2014). The effects of the monetary policy stance on the transmission mechanism. *Studies in Nonlinear Dynamics & Econometrics 18*(3), 217–236.

Garín, J., R. Lester, and E. Sims (2019). Are supply shocks contractionary at the zlb? evidence from utilization-adjusted tfp data. *Review of Economics and Statistics 101*(1), 160–175.

Girosi, F. and T. Poggio (1990). Networks and the best approximation property. *Biological Cybernetics 63*(3), 169–176.

Guerrón-Quintana, P. and M. Zhong (2017). Macroeconomic forecasting in times of crises.

Guresen, E., G. Kayakutlu, and T. U. Daim (2011). Using artificial neural network models in stock market index prediction. *Expert Systems with Applications 38*(8), 10389–10397.

Hamilton, J. D. (1989). A new approach to the economic analysis of nonstationary time series and the business cycle. *Econometrica*, 357–384.

Härdle, W., H. Lütkepohl, and R. Chen (1997). A review of nonparametric time series analysis. *International Statistical Review 65*(1), 49–72.

Härdle, W. and A. Tsybakov (1997). Local polynomial estimators of the volatility function in nonparametric autoregression. *Journal of Econometrics 81*(1), 223–242.

Härdle, W., A. Tsybakov, and L. Yang (1998). Nonparametric vector autoregression. *Journal of Statistical Planning and Inference 68*(2), 221–245.

Hartman, E. J., J. D. Keeler, and J. M. Kowalski (1990). Layered neural networks with gaussian hidden units as universal approximations. *Neural Computation 2*(2), 210–215.

Hubrich, K. and T. Teräsvirta (2013). Thresholds and smooth transitions in vector autoregressive models. In *VAR Models in Macroeconomics–New Developments and Applications: Essays in Honor of Christopher A. Sims*, pp. 273–326. Emerald Group Publishing Limited.

Hutchinson, J. M., A. W. Lo, and T. Poggio (1994). A nonparametric approach to pricing and hedging derivative securities via learning networks. *Journal of Finance 49*(3), 851–889.

Jeliazkov, I. (2013). Nonparametric vector autoregressions: Specification, estimation, and inference. In *VAR Models in Macroeconomics–New Developments and Applications: Essays in Honor of Christopher A. Sims*, pp. 327–359. Emerald Group Publishing Limited.

Jordà, Ò. (2005). Estimation and inference of impulse responses by local projections. *American Economic Review 95*(1), 161–182.

Kilian, L. (2008). Exogenous oil supply shocks: How big are they and how much do they matter for the us economy? *Review of Economics and Statistics 90*(2), 216–240.

Koop, G. and D. Korobilis (2013). Large time-varying parameter vars. *Journal of Econometrics 177*(2), 185–198.

Koop, G., D. Korobilis, et al. (2010). Bayesian multivariate time series methods for empirical macroeconomics. *Foundations and Trends® in Econometrics 3*(4), 267–358.

Koop, G., R. Leon-Gonzalez, and R. W. Strachan (2009). On the evolution of the monetary policy transmission mechanism. *Journal of Economic Dynamics and Control 33*(4), 997–1017.

Koop, G., M. H. Pesaran, and S. M. Potter (1996). Impulse response analysis in nonlinear multivariate models. *Journal of Econometrics 74*(1), 119–147.

Koop, G. and S. M. Potter (2007). Estimation and forecasting in models with multiple breaks. *The Review of Economic Studies 74*(3), 763–789.

Krolzig, H.-M. (2013). *Markov-switching vector autoregressions: Modelling, statistical inference, and application to business cycle analysis*, Volume 454. Springer Science & Business Media.

Kuan, C.-M. and H. White (1994). Artificial neural networks: An econometric perspective. *Econometric Reviews 13*(1), 1–91.

Lachtermacher, G. and J. D. Fuller (1995). Back propagation in time-series forecasting. *Journal of Forecasting 14*(4), 381–393.

Maliar, L. and S. Maliar (2015). Merging simulation and projection approaches to solve high-dimensional problems with an application to a new keynesian model. *Quantitative Economics 6*(1), 1–47.

Moody, J. and C. J. Darken (1989). Fast learning in networks of locally-tuned processing units. *Neural Computation 1*(2), 281–294.

Moshiri, S. and N. Cameron (1999). Neural network versus econometric models in forecasting inflation.

Park, J. and I. W. Sandberg (1991). Universal approximation using radial-basis-function networks. *Neural Computation 3*(2), 246–257.

Pesaran, M. H. and Y. Shin (1996). Cointegration and speed of convergence to equilibrium. *Journal of Econometrics 71*(1), 117–143.

Petrova, K. (2019). A quasi-bayesian local likelihood approach to time varying parameter var models. *Journal of Econometrics 212*(1), 286–306.

Poggio, T. and F. Girosi (1990). Networks for approximation and learning. *Proceedings of the IEEE 78*(9), 1481–1497.

Potter, S. M. (1995). A nonlinear approach to us gnp. *Journal of Applied Econometrics 10*(2), 109–125.

Potter, S. M. (2000). Nonlinear impulse response functions. *Journal of Economic Dynamics and Control 24*(10), 1425–1446.

Primiceri, G. E. (2005). Time varying structural vector autoregressions and monetary policy. *The Review of Economic Studies 72*(3), 821–852.

Ramey, V. A. (2011). Identifying government spending shocks: It's all in the timing. *The Quarterly Journal of Economics 126*(1), 1–50.

Robinson, P. M. (1983). Nonparametric estimators for time series. *Journal of Time Series Analysis 4*(3), 185–207.

Romer, C. D. and D. H. Romer (2004). A new measure of monetary shocks: Derivation and implications. *American Economic Review*, 1055–1084.

Romer, C. D. and D. H. Romer (2010). The macroeconomic effects of tax changes: Estimates based on a new measure of fiscal shocks. *American Economic Review 100*, 763–801.

Rothman, P., D. Van Dijk, and P. Hans (2001). Multivariate star analysis of money–output relationship. *Macroeconomic Dynamics 5*(4), 506–532.

Sims, C. A., D. F. Waggoner, and T. Zha (2008). Methods for inference in large multiple-equation markov-switching models. *Journal of Econometrics 146*(2), 255–274.

Sims, C. A. and T. Zha (1998). Bayesian methods for dynamic multivariate models. *International Economic Review 39*(4), 949–68.

Sims, C. A. and T. Zha (2006). Were there regime switches in us monetary policy? *American Economic Review 96*(1), 54–81.

Swanson, N. R. and H. White (1997). A model selection approach to real-time macroeconomic forecasting using linear models and artificial neural networks. *Review of Economics and Statistics 79*(4), 540–550.

Teräsvirta, T., D. Tjøstheim, C. W. J. Granger, et al. (2010). *Modelling nonlinear economic time series*. Oxford University Press Oxford.

Tkacz, G. (2001). Neural network forecasting of canadian gdp growth. *International Journal of Forecasting 17*(1), 57–69.

Wieland, J. F. (2019). Are negative supply shocks expansionary at the zero lower bound? *Journal of Political Economy 127*(3), 973–1007.

Xu, L., A. Krzyżak, and A. Yuille (1994). On radial basis function nets and kernel regression: Statistical consistency, convergence rates, and receptive field size. *Neural Networks 7*(4), 609–628.

Zhang, G. and M. Y. Hu (1998). Neural network forecasting of the british pound/us dollar exchange rate. *Omega 26*(4), 495–506.

Zhang, Y.-Q. and X. Wan (2007). Statistical fuzzy interval neural networks for currency exchange rate time series prediction. *Applied Soft Computing 7*(4), 1149–1156.